Universidade de Lisboa

Faculdade de Ciências

Departamento de Física

Predicting muscle fibre type composition through joint mechanics

Ana Catarina Valente Ferreira

Dissertação da Tese de Mestrado

Mestrado Integrado em Engenharia Biomédica e Biofísica
Perfil de Engenharia Clínica e Instrumentação

Ano 2012

Universidade de Lisboa

Faculdade de Ciências

Departamento de Física

Predicting muscle fibre type composition through joint mechanics

Ana Catarina Valente Ferreira

Dissertação da Tese de Mestrado orientada por:
Prof. Doutor Hugo Ferreira
Prof. Doutor Erwin de Vlugt

Mestrado Integrado em Engenharia Biomédica e Biofísica

Ano 2012

Abstract

Ageing, neurological diseases or certain conditions can result in changes in muscle properties, such as fibre type composition, which may influence muscle performance. Short-range stiffness (SRS) is a mechanical property of muscles which reflects mainly the stiffness of the attached cross-bridges. Different fibre types are believed to have different SRS and thus SRS might be important in characterizing muscle fibre type composition. Recently, a model-based estimation method was developed to estimate wrist muscles SRS *in vivo*.

In this study, the same method was used to estimate leg muscles SRS using an ankle manipulator. Subjects (n=10) were measured with the leg extended and flexed at 90° at five torque levels, ranging from 0 to 20 Nm. It was expected that with the knee extended the recruitment of type II fibres would be greater at higher torques and thus, the estimated SRS would be lower. Two subjects were measured on different days for repeatability analysis. Furthermore, a geometrical model was developed to predict the contribution of tendon stiffness and muscle pennation angle to SRS.

From the simulation results, the SRS model developed for the wrist seems adequate to estimate leg muscles SRS. However, some of the model parameters presented high standard error mean (SEM) values as well as high inter-trial standard deviations (ITSTD). Improvements in the equipment and in the attachment between the foot and the footplate might be necessary to confirm the goodness of the model fit. Regarding the estimated SRS at different knee angles, no significant differences were found. From the sensitivity analysis of the geometrical model, tendon stiffness seems to have a large influence on muscle stiffness and thus its inclusion in the SRS model should be considered.

Key-words: fibre type, *in vivo* estimation, short-range stiffness, leg muscles, knee angle

Sumário

O envelhecimento, doenças neurológicas ou determinadas condições, como a imobilização prolongada, podem resultar em alterações nas propriedades das fibras musculares, como a composição a nível do tipo de fibras, o que pode influenciar o desempenho muscular. Acredita-se ainda que o treino físico específico pode fazer regredir estas alterações. Existe assim uma necessidade de quantificar estas alterações que ocorrem nos músculos, de modo a fazer um diagnóstico, *follow up* e reabilitação dos pacientes mais adequados. Actualmente, o método padrão para estimar a composição das fibras musculares implica a realização de biópsias, o que é invasivo e desconfortável para os pacientes. Desta forma, existe a necessidade de desenvolver métodos não invasivos que permitam avaliar quantitativamente as propriedades dos músculos.

Os músculos são constituídos por diversos fascículos que englobam várias fibras musculares. Por sua vez, as fibras do músculo esquelético englobam várias miofibrilas, que resultam da repetição em série de sarcómeros. Cada sarcómero é principalmente constituído por dois filamentos, a miosina e a actina, que se ligam formando *cross-bridges*. Durante a contracção muscular, ocorre um deslizamento dos filamentos entre si, fenómeno responsável pela geração da força muscular. De forma geral, existem dois tipos de fibras principais: as fibras de contracção lenta ou do tipo I e as fibras de contracção rápida ou do tipo II. Acredita-se que as fibras do tipo II têm capacidade de gerar uma maior potência a velocidades mais elevadas, comparando com as fibras do tipo I, e portanto pensa-se que são preferencialmente recrutadas em movimentos rápidos e/ou que exijam um esforço mais elevado.

A *short-range stiffness* (SRS) é uma propriedade mecânica das fibras do músculo esquelético que reflecte maioritariamente a resistência das *cross-bridges*. Esta propriedade manifesta-se quando uma fibra muscular se encontra num determinado estado de contracção e é rapidamente alongada. Considerando experiências efectuadas em unidades musculares inteiras, a SRS é influenciada por outros factores, tais como a resistência dos tendões e das aponevroses. Acredita-se ainda que os diferentes tipos de fibras musculares, tipo I e tipo II, possuem diferentes SRS. Esta propriedade foi descoberta a partir de experiências realizadas com fibras dissecadas de animais e posteriormente

explorada em experiências utilizando músculos inteiros de animais. Utilizando técnicas de modelação e estimação de pârametros, é possível estimar as propriedades mecânicas dos músculos a partir de medições efectuadas ao nível das articulações. Recentemente, foi desenvolvido um método para estimar a SRS dos músculos flexores e extensores do punho *in vivo*. Este método envolve a utilização de um manipulador háptico que permite aplicar rotações rápidas à articulação do pulso, no sentido contrário àquele em que o sujeito está a gerar uma determinada força. Através da deslocação e do momento de força medidos durante os primeiros 40 ms da rotação, e utilizando um modelo mecânico adequado, é possível então estimar a SRS dos músculos envolvidos.

O principal objectivo deste estudo foi verificar se o modelo desenvolvido para o pulso seria adequado para determinar a SRS dos músculos da perna, utilizando um manipulador para o tornozelo. Outro objectivo foi determinar se a SRS dos músculos da perna é influenciada pelo grau de flexão da perna utilizada durante a experiência. Assumindo que os músculos da perna, em particular os flexores plantares, possuem diferentes composições a nível do tipo de fibras musculares, estas diferenças poderão ser detectadas estimando a SRS com a perna posicionada com diferentes ângulos do joelho. Isto porque se acredita que, quando o joelho está flectido, a capacidade de gerar força do músculo *gastrocnemius*, que possui uma maior quantidade de fibras do tipo II do que os outros músculos flexores plantares, é reduzida. Desta forma, considerando que com a perna estendida, o recrutamento de fibras do tipo II é superior ao que se consegue com a perna flectida, espera-se que a SRS seja inferior com a perna estendida, assumindo que as fibras do tipo II possuem uma menor SRS do que as fibras do tipo I. Para além disso, foi desenvolvido um modelo geométrico a fim de prever se o ângulo de penação, isto é, o ângulo entre as fibras musculares e as aponevroses, e a resistência do tendão influenciam, de forma significativa, a SRS estimada, dado que os músculos da perna considerados são penados e estes parâmetros não estão incluídos no modelo usado para estimar a SRS.

O protocolo para estimar a SRS consiste em gerar um determinado momento de força no manipulador para o tornozelo, na direcção de flexão plantar, aplicando-se em seguida uma rotação na direcção oposta, com cerca de 8.6° de amplitude e uma velocidade máxima de 2 rad/s. Os participantes (n=10) recrutados para esta experiência eram jovens adultos do sexo masculino, com idades compreendidas entre os 24-51 anos, e tinham que gerar 5 momentos, entre os 0 e os 20 Nm. No caso de 0 Nm, foi pedido aos participantes que relaxassem e a rotação era aplicada automaticamente. A ordem dos momentos era aleatória e para cada momento foram realizadas três repetições. As medições foram efectuadas na perna esquerda, nas posições estendida (180°) e flectida (90°), para todos os participantes. Dois dos participantes repetiram as medições num

dia diferente para efeitos de análise de repetibilidade do método.

Nas simulações do modelo da SRS obtidas com os dados dos participantes, é possível observar um ponto de transição no momento elástico do tornozelo em função do tempo e da deslocação angular do tornozelo. Estes resultados são semelhantes aos obtidos para o pulso e pensa-se que esta descontinuidade resulta da transição da resistência dos músculos de um valor elevado, correspondente à SRS, para um valor inferior. Assim, este modelo parece adequado para estimar a SRS dos músculos da perna. No entanto, apesar dos elevados valores da variância entre os momentos medidos e estimados (VAF) das simulações, alguns dos parâmetros do modelo apresentaram um elevado erro padrão da média (SEM) e um elevado desvio padrão entre repetições (ITSTD), o que significa que não foram estimados com grande precisão. Para além disso, os parâmetros estimados para os dois participantes, medidos em dias diferentes, apresentaram um variabilidade considerável. No entanto, um dos participantes utilizou um suporte de fixação adicional no pé no segundo dia, o que poderia explicar estas diferenças.

Como esperado, observou-se um aumento da SRS com o momento de força, principalmente devido ao aumento do número de *cross-bridges*, assumindo que a força gerada por cada *cross-bridge* é constante. No entanto, não foram encontradas diferenças significativas entre a SRS estimada a partir das medições efectuadas com o joelho estendido e com o joelho flectido. É importante notar que os participantes geraram momentos de força bastante inferiores ao momento máximo de contracção voluntária (MVC) normalmente encontrado para jovens do sexo masculino, que é superior a 100 Nm. Assim, os momentos gerados podem não ter sido suficientemente elevados para que houvesse um recrutamento significativo de fibras do tipo II, o que poderia explicar o facto de não terem sido encontradas diferenças significativas na SRS estimada para diferentes ângulos do joelho.

Em relação aos resultados da análise sensitiva efectuada com o modelo geométrico, o parâmetro que parece ter maior influência na SRS é a resistência do tendão, seguido do comprimento do braço do momento de forças. O ângulo de penação parece não ter uma influência significativa (cerca de 5%) na SRS, considerando momentos de força até aos 20 Nm. Estes resultados sugerem que poderia ser conveniente adicionar um componente ao modelo da SRS para representar a resistência do tendão. Esta pode ser estimada a partir do alongamento do tendão, que pode ser medida através da utilização de ultrassons.

No sentido de confirmar os resultados deste estudo, é necessário efectuar alguns aperfeiçoamentos no equipamento. Um aumento da rigidez da plataforma do manipulador, onde é colocado o pé, e uma melhor ligação entre o pé e a plataforma poderiam melhorar os resultados das simulações do modelo da SRS, especialmente a estimação

dos parâmetros do manipulador, que registaram valores baixos para a VAF e foram ajustados aquando a análise dos dados dos participantes. Para além disso, seria importante aumentar a potência do manipulador, o que permitiria medir o momento de MVC de cada participante, estimar a SRS gerando momentos mais elevados e aplicar rotações com maior velocidade, um factor que pode ser determinante na estimação da SRS. De facto, no estudo realizado no pulso foram utilizadas rotações com uma velocidade máxima de cerca de 3 rad/s e neste estudo a velocidade estava limitada a 2 rad/s, atingindo valores máximos inferiores a 1.5 rad/s quando os sujeitos geravam momentos de 20 Nm. Outra melhoria que podia ser feita a nível do modelo da SRS, seria a discriminação dos diferentes músculos que contribuem para a SRS, como sugerido anteriormente no estudo do pulso.

A hipótese de que a SRS pode ser utilizada para prever a composição do tipo de fibras dos músculos envolvidos necessita de uma maior investigação. O mesmo tipo de medições poderia ser efectuado utilizando momentos de força mais elevados e aplicando rotações com maior velocidade. Poderiam também ser explorados diferentes tipos de protocolos, no sentido de dar ênfase a outras propriedades que distinguem as fibras musculares, como a resistência à fadiga e a potência gerada. No futuro, poderiam ainda ser investigados grupos de participantes idosos, pacientes que estiveram imobilizados durante um determinado tempo ou pacientes que foram sujeitos a um treino físico específico pois, tal como referido anteriormente, acredita-se que estes indivíduos sofrem alterações a nível da composição do tipo de fibras musculares. Seria ainda interessante investigar grupos de pacientes com alterações a nível da resistência dos tendões ou pacientes com um historial de quedas, dado que a SRS parece ser importante na recuperação do equilíbrio após perturbações rápidas a nível das articulações.

Palavras-chave: tipos de fibras musculares, estimação *in vivo*, *short-range stiffness*, músculos da perna, ângulo do joelho

Acknowledgements

I wish to thank, first and foremost, Professor Erwin de Vlugt, from the Technical University of Delft, for giving me the opportunity to develop my project in the Netherlands. Professor Erwin de Vlugt and Professor Jurriaan de Groot, from the Leids Universitair Medisch Centrum (LUMC), gave me continued support and motivation and without their expertise and patience this thesis would not be possible.

Secondly, I acknowledge Professor Hugo Ferreira for accepting to be my supervisor and for the help and motivation, specially in the last phase of the project.

I would also like to express my gratitude to all the people involved from the Rehabilitation Department and the Biomechanics Laboratory of the LUMC, specially Stijn Eesbeek who shared his knowledge and work with me. In addiction, I would like to thank to all the co-workers for contributing to a very friendly working environment and for participating in my experiment.

I owe sincere and earnest thankfulness to my parents not only for the financial support, which made this project possible, but also for their endless support and encouragement throughout my whole academic life. Last but not least important, I would like to thank my friends who supported me during the entire project, in particular David Leffler.

Contents

List of Figures

List of Tables

List of Symbols and Abbreviations

α	muscle pennation angle
θ	ankle angle (angle between the sole foot and the tibia)
$\theta_{m,sim}$	simulated angular displacement
θ_m	measured angular displacement of the footplate
b_f	foot-manipulator interface damping
b_j	joint damping
b_l	manipulator damping
I_j	joint inertia
I_l	manipulator inertia
k_f	foot-manipulator interface stiffness
k_j	joint stiffness
k_l	manipulator stiffness
k_m	muscle stiffness
k_t	tendon stiffness
k_{dec}	stiffness beyond elastic limit (decrement to k_{SRS})
$k_{m,eq}$	muscle effective stiffness
k_{SRS}	estimated short-range stiffness (SRS)
L_s	sarcomere length
L_{MTU}	muscle tendon-unit length

r	muscle moment arm length
T	ankle torque
T_l	measured torque on the footplate
$T_{j,elas}$	elastic part of the simulated joint torque
$T_{l,f}$	filtered measured torque
$T_{l,sim}$	simulated measured torque
x_e	elastic limit (joint angle at which k_j changes)
x_s	elastic limit in nm p.h.s.
ATP	adenosine triphosphate
ATPase	adenosine triphosphatase
EMG	electromyography/electromyographic
FF	fast fibres
GL	gastrocnemius lateralis muscle
GM	gastrocnemius medialis muscle
ITSTD	inter-trial standard deviation
MHC	myosin heavy chain
MN	motor neuron
MRS	magnetic resonance spectroscopy
MTC	muscle-tendon complex
MU	motor unit
MVC	maximum voluntary contraction
p	p-value
p.h.s.	per half sarcomere
RP	muscle responsive power

SDH	succinate dehydrogenase
SEM	Standard Error of the Mean
SF	slow fibres
SIPE	system identification and parameter estimation
SOL	soleus muscle
SRS	short-range stiffness
TA	tibialis anterior muscle
TMG	tensiomyography
TS	triceps surae muscles (composed by GM, GL and SOL muscles)
VAF	Variance Accounted For

Chapter 1

Introduction

Skeletal muscle properties are determinant in joint movements and they can be estimated *in vivo* through the use of powerful haptic manipulators and modelling techniques. The aim of this study is to determine leg muscles short-range stiffness (SRS) from the ankle joint mechanics. This parameter might reflect fibre type composition of leg muscles, an important property of skeletal muscle which can only be assessed through invasive methods currently.

This chapter describes skeletal muscle function and organization, the current methods of muscle fibre typing, muscle mechanical properties related to fibre type and how it is possible to estimate these properties by measuring joint mechanics.

1.1 Skeletal muscle function and organization

Skeletal muscle is attached to bones via tendons and its contraction results in joint motion. Muscles are composed of fascicles which enclose several fibres. Muscle fibres comprise many myofibrils with a banding pattern formed by the repetition of sarcomeres in series along the length of the myofibrils. Each sarcomere is mainly composed of thick filaments (myosin) and thin filaments (actin) that overlap, as represented in figure 1.1. According to the cross-bridge theory, in the presence of calcium and adenosine triphosphate (ATP), myosin heads attach to actin and a power stroke occurs resulting in a sliding of the thick filament over the thin filament. This event propagates to the adjacent sarcomeres and muscle fibres shorten giving rise to a force which is transmitted to the tendons according to the muscle architecture, i.e. muscle pennation angle. At the joint level, this force is responsible for the limb rotation. Skeletal muscle fibres are stimulated to contract by motor neurons (MNs). The functional unit of skeletal muscle is the motor unit (MU), which is composed by a MN and the group of muscle fibres it innervates.

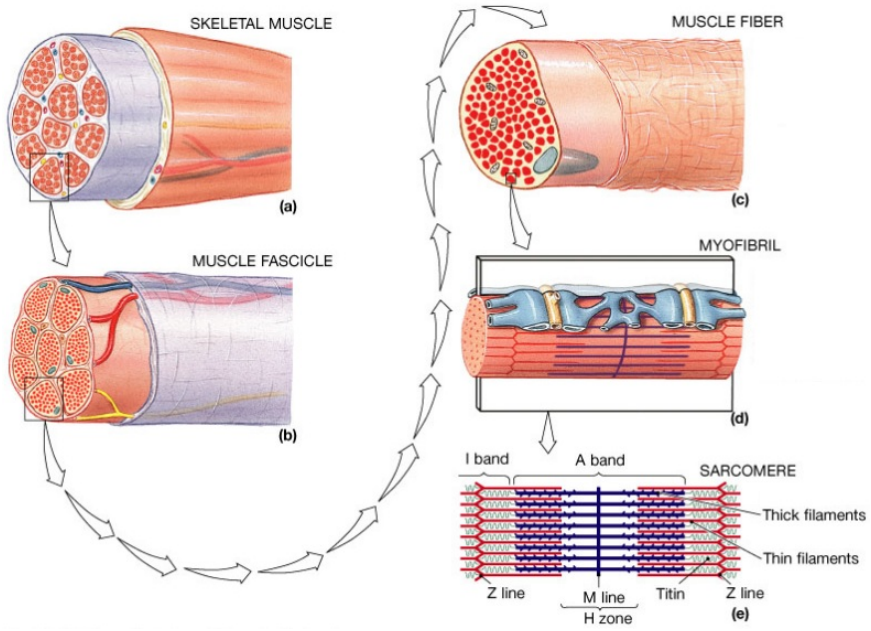

Figure 1.1: Representation of the different levels of organization of the skeletal muscle. (a) Skeletal muscle encloses several (b) fascicles which are composed of (c) muscle fibres. Each muscle fibre contains several (d) myofibrils which consist of (e) sarcomeres, the structural unit of skeletal muscle. Each sarcomere contains thick (myosin) and thin (actin) filaments which connect and slide over each other producing force. Figure modified from `http://faculty.sdmiramar.edu/kpetti/bio160/documents%20biol160.htm`.

Muscle fibres have different properties and thus muscle performance depends, amongst other factors, on the content of muscle fibre types. It is believed that each MU is composed of fibres with similar phenotypes. This organization of the MUs and the muscle heterogeneity allows the specific recruitment of certain fibre types so that muscle performance adapts to tasks with different functional demands. This also means that fibres of the same type are associated with MNs with similar firing patterns and hence, the diversity of muscle fibre types can be explained as a result of their adaptation to different neural activity. Fibre type diversification can also result from an adaptation to whole body metabolism as skeletal muscle is responsible for proteins storage and glucose absorption [1].

Muscle fibres plasticity, i.e. transitions from one type to another, is an important feature of muscle function because it has consequences on the mechanical and energy expenditure properties of muscles. Muscle fibre type composition can change in turn due to diseases, such as type 2 diabetes [2, 3], or determined conditions, like prolonged immobilization [4, 5], specific exercise training [6, 7, 8, 9] and ageing [10, 11, 12, 13]. This changes may be due to conversion of muscle fibres types to another but also due to a selective atrophy of certain populations of muscle fibre types [11].

With ageing, these changes can be related to a decreased capacity of the elderly

to generate fast movements which is crucial to regain balance after a disturbance and prevent falling. Therefore, estimation of muscle fibre type content is important to monitor muscle changes and develop effective physical therapies. Moreover, it may contribute to evaluate muscle transitions due to determined diseases or conditions, previously described.

1.2 Current methods of muscle fibre typing

Skeletal muscle is described as having two main types of fibres: type I or slow (SF) and type II or fast fibres (FF), which were originally classified according to their different speed of contraction and appearance [1, 11]. SF have a red appearance while FF have a white appearance due to lower amounts of haemoglobin and lower capillary contents [11].

Currently, the most common methods of fibre typing are based on the histochemical or immunohistochemical analysis of muscle samples. Myosin adenosine triphosphatase (ATPase) staining relies on the different rate of ATP consumption which is higher for FF [14, 11]. Succinate dehydrogenase (SDH) staining, another common method, is based on the detection of SDH, an enzyme located at the mithocondria which is related to the fatigue resistance properties of muscle fibres. It was found that SF and certain FF, believed to correspond to type IIA fibres, were more resistant to fatigue than type IIB fibres, which contain a higher content of glycolytic enzymes [14, 11]. More recently, a third method was developed based on myosin heavy chain (MHC) identification using antimyosin antibodies or electrophoretic separation which allows a more accurate identification of fibre subtypes and the existence of 'hybrid' fibres, i.e. fibres expressing more than one myosin isoform [14, 11]. This is a strong evidence of muscle heterogeneity and supports the idea that muscle fibres can convert from one type to another in response to hormonal and, mainly, neural influences allowing for muscle fibres adaptation to different functional demands [1, 11].

Although all these classification methods are considerably reliable, they involve doing muscle biopsies, which is a local invasive procedure, and the results are only representative of the whole muscle being analysed. Furthermore, histochemical methods mainly provide information about the energy consumption of muscle fibres but not about their mechanical behaviour. Consequently, there is a need to develop a reliable non-invasive method for *in vivo* muscle fibre typing at the functional joint level which provides information about whole muscle mechanics.

In the past decade, different non-invasive techniques, like magnetic resonance imaging (MRI) [15], magnetic resonance spectroscopy (MRS) [10] and tensiomyography

(TMG) [16] have been studied for this purpose. Although some of these methods have shown potential, more research is needed and thus none of them is clinically available yet.

1.3 Muscle mechanics

Besides different chemical and molecular properties, muscle fibre types also differ in mechanical properties. Dissection of single muscle fibres allowed the study of mechanical and other properties of different fibre types in vitro. In terms of power and velocity, FF can develop a higher power at a lower velocity comparing to SF [14], as it can be observed in figure 1.2. However, this method presents the same limitations as the previous methods described since it also implies doing local muscle biopsies.

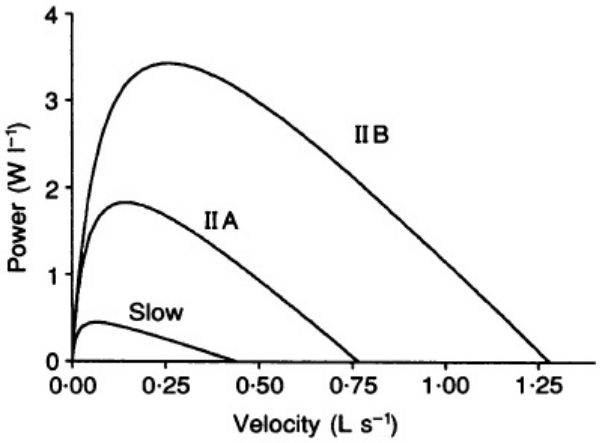

Figure 1.2: Power-velocity curves of the different human fibre types calculated from Hill's hyperbolic equation used to fit experimental force-velocity curves. SF refer to type I fibres and type IIA and IIB correspond to subtypes of FF. Muscle fibres were obtained from the vastus lateralis muscle, analysed by load-clamp manoeuvres at 12°C and characterized on the basis of the MHC isoform composition by SDH-polyacrylamide gel electrophoresis. Power is expressed in Watts per litre (W/l), equivalent to $1{\times}10^3$ newton per second squared meter ($N/(sm^2)$), and velocity in fibre segment length per second (L/s). Figure taken from [17].

Another important mechanical property of muscle fibres is SRS. When a contracting muscle is stretched or concentrically shortened there is an initial steep rise or an initial steep fall in tension, respectively. This tension change divided by the length change is referred to as SRS, as illustrated in figure 1.3. If the velocity of the stretch is sufficiently high, SRS is thought to be due to deformation of existing cross-bridges without significant break down or reattachment [18]. Therefore, SRS depends on the activation level of the muscle, i.e. number of cross-bridges attached, and hence to the tension level prior to the stretch [19]. When measuring SRS of the whole tendon-muscle unit, SRS can be influenced by passive structures connected in series with the cross-

bridges force transfer pathway, such as the tendon and connective tissue. SRS may be affected by other parameters as well, such as muscle architecture [19]. Since SRS occurs prior to reflex responses, it may have an important role in balance maintenance after rapid perturbations [18].

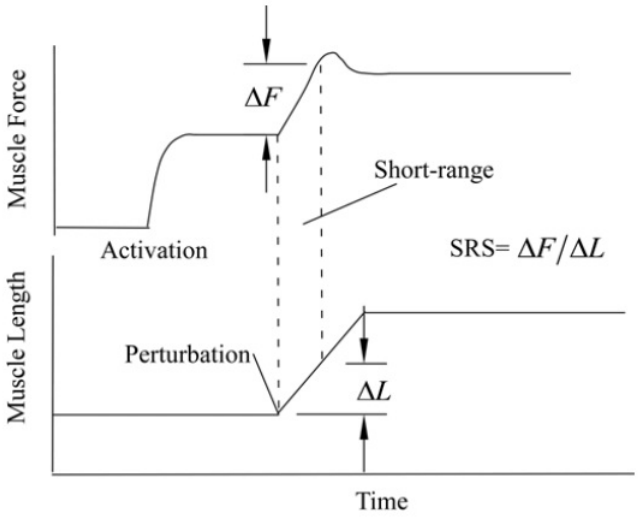

Figure 1.3: Short-range stiffness (SRS) is defined as the ratio between the initial force change (ΔF) and the length change (ΔL) after applying a fast ramp stretch to a contracting muscle. Figure taken from [20].

Regarding fibre type composition, studies on isolated muscle fibres and single MUs suggested that SF are stiffer than FF [21, 22, 23]. Gregory et. al [24] suggested that this difference in SRS between SF and FF could be explained by differences in fibre length. More recently, SRS was measured at the whole muscle level and no significant differences were found in SRS of muscles with different fibre type composition [25] or these could be explained by differences in fibre length [26].

1.4 From joint mechanics to muscle properties

Joint mechanics can provide information about muscle performance *in vivo* and thus they may reflect the mechanical differences between fibre types. Using powerful and precise haptic manipulators [27], it is possible to apply perturbations to a certain joint and measure the changes in the joint position and torque, which is mainly determined by the muscle force delivered by the tendons to the joint. An haptic device can change its mechanical properties under computer control and according to the user's behaviour. Therefore, it receives feedback from the user and generates mechanical signals that stimulate the user [28]. For example, an haptic manipulator for the ankle can behave as a mass-spring-damper system whose inertia, stiffness and damping are computer

controlled to create different environments with which the user will interact. Later on, it is possible to estimate muscle properties, such as generated power and intrinsic stiffness, by using system identification and parameter estimation (SIPE) techniques. The main advantages of this method is that it is non-invasive, it can be used repeatedly, without discomfort for the patients, and it provides information about the mechanics of the whole muscles that contribute to the joint stabilization and joint mechanics in general. On the other hand, this method implies that the user has a certain mobility and capacity to generate force.

Eesbeek et. al [29] developed a mechanical model to estimate muscle SRS from the first 10-40 ms of the measured torque after applying fast stretches to the joint with an haptic manipulator. It was possible to observe a discontinuous derivative in the elastic joint torque plotted against time and joint position, as shown in figure 1.4(a). This discontinuity is believed to be due to the initial high muscle stiffness (SRS) followed by a decline. Similar results were observed in muscle tension changes with length on experiments done with single muscle fibres [21], as represented in figure 1.4(b).

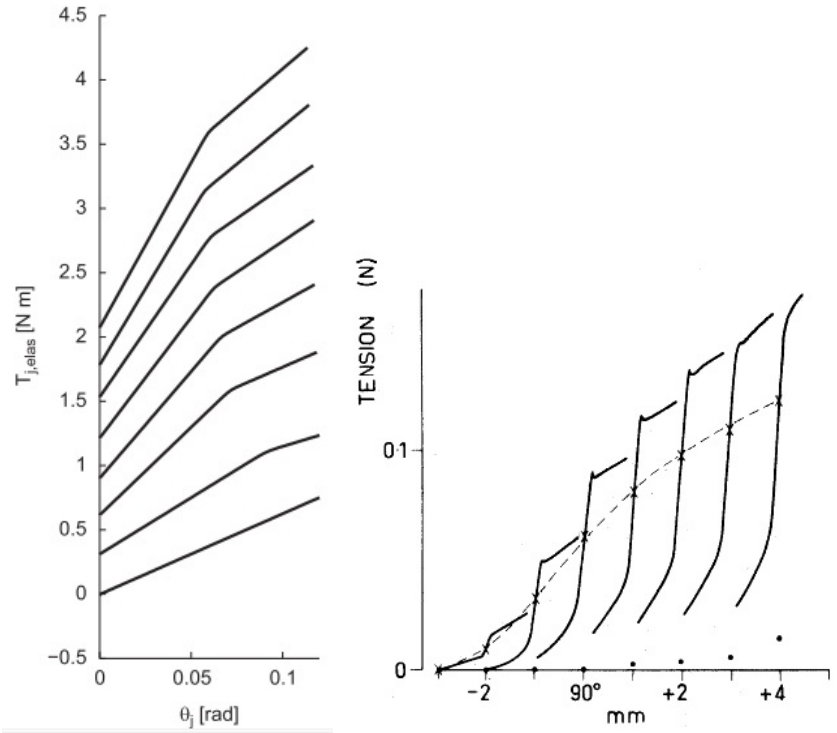

(a) (b)

Figure 1.4: (a) Estimated elastic wrist joint torque ($T_{j,elast}$) as function of time wrist displacement (θ_j). Figure taken from [29]. (b) Muscle fibre tension change as a function of fibre length. Figure taken from [21]. In both plots it is possible to observe a corner associated with the transition of muscle SRS to a lower value.

The model developed by Eesbeek et. al [29] consists of three mechanical subsystems as represented in figure 1.5. The subsystem I represents the mechanical properties of the

manipulator and is composed by the manipulator inertia (I_l), stiffness (k_l) and damping (b_l). The subsystem II describes the interface between the manipulator footplate and the foot and is composed by two elements, a stiffness (k_f) and a damping (b_f). The subsystem III represents the joint mechanics and it consists of an inertia (I_j), a stiffness (k_j) and a damping element (b_j). The joint stiffness (k_j) is modelled has having a bi-phasic behaviour, i.e. an initial high stiffness (corresponding to muscle SRS, k_{SRS}) followed by a decline (k_{dec}) that occurs at a determined joint position, the elastic limit (x_e). The model is described in more detail in appendix A.

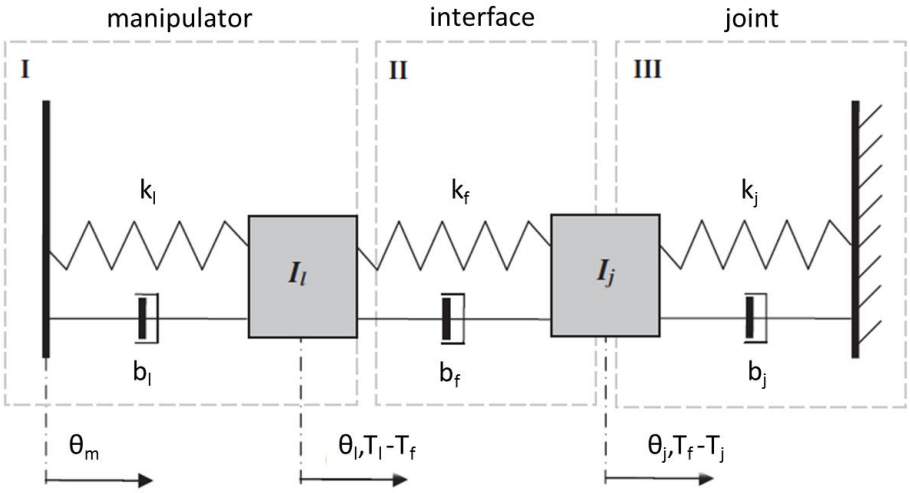

Figure 1.5: Mechanical model used to estimate muscle SRS from joint mechanics. Figure modified from [29].

More recently, Stijntjes [30] calculated the SRS of the wrist flexors of young and older subjects using the same model. In this study, muscle responsive power (RP) was also estimated, using a similar mechanical model. Subjects were asked to generate a certain torque on an haptic manipulator, as in the SRS protocol, and the handle was suddenly released. During the first 40-50 ms the muscles extended and exerted a certain power which was defined as the RP. The maximal RP and the velocity at which it happens is thought to be related to the turn-over rate of the cross-bridges as SRS. No age related differences were found in these parameters, as expected, but the significant differences found between male and female subjects suggested that these parameters could be related to differences in muscle fibre type composition. In figure 1.6 it is possible to observe an example of power-velocity curves estimated for young and old subjects and the results obtained for SRS.

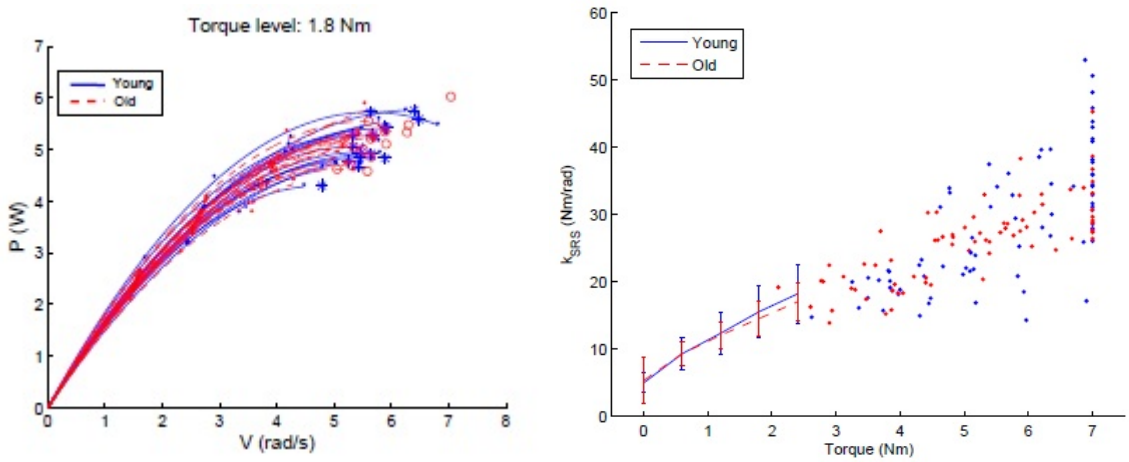

(a) (b)

Figure 1.6: (a) Power-velocity curves at a torque level of 1.8 Nm for young (blue solid lines) and old (red dashed line) subjects. Curves were fitted through real measurement (dots) of peak muscle power at different viscous loads. Maximal RP is indicated by asterisks (young subjects) and circles (old subjects). (b) Mean k_{SRS} (SRS) of the wrist and respective standard deviation of young (blue solid line) and old (red dashed line) subjects at different torque levels. Values of repeated measurements were averaged over subjects between torque levels of 0 and 2.4 Nm. For higher torque levels (60% and 80% of maximal voluntary contraction), repeated measurements are plotted separately (dots). It is possible to observe the approximately linear increase in SRS with torque level which is believed to be mainly due to an increase in the number of cross-bridges attached. Figures taken from [30].

1.5 Leg muscles

Leg muscles have been widely studied either *in vitro* or *in vivo* due to their importance in daily activities, such as gait. The main leg muscles that contribute to ankle torque are soleus (SOL), tibialis anterior (TA) and gastrocnemius, which is composed by two heads, gastrocnemius medialis (GM) and gastrocnemius lateralis (GL). Gastrocnemius and SOL are often referred to as triceps surae (TS) and are the main plantar flexors, i.e. the main muscles that contribute to generate a torque in the plantarflexion direction. Plantarflexion occurs when the ankle rotates and the foot moves downwards toward the sole. Dorsiflexion refers to the movement of the foot in the opposite direction. The main dorsiflexor, i.e. the main muscle that opposes plantarflexion, is TA. These muscles are illustrated in figure 1.7.

Comparing to the wrist muscles, leg muscles have different properties regarding muscle fibre type composition and muscle architecture. In terms of muscle fibre type composition, while SOL is predominantly composed by SF or type I fibres, gastrocnemius has a greater amount of FF or type II fibres [16, 32]. Regarding muscle architecture, gastrocnemius, SOL and TA are pennated muscles, i.e. muscle fibres are not arranged in parallel in relation to the aponeurosis as represented in figure 1.8. Gastrocnemius is both inserted on the knee and ankle joints and thus with increasing

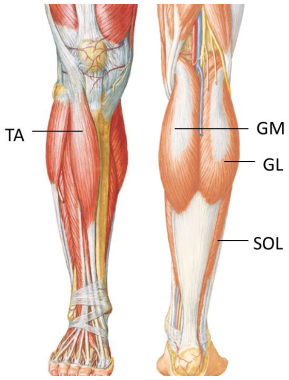

(a) (b)

Figure 1.7: (a) Anterior view of the human leg, where the muscle tibialis anterior (TA), the main contributor to ankle dorsiflexion, can be observed. (b) Posterior view of the human leg. It is possible to observe both gastrocnemius heads, gastrocnemius medialis (GM) and gastrocnemius lateralis (GL), and soleus (SOL), the main contributors to ankle plantarflexion. Figures taken from [31].

knee flexion, and with increasing contraction level, fibre length decreases and pennation angle increases, while SOL architecture remains approximately constant [33, 34]. Moreover SOL, gastrocnemius and TA are believed to work on the ascending limb of their force-length relationships [35, 36, 37], which means that their force production is greater at longer fibre lengths.

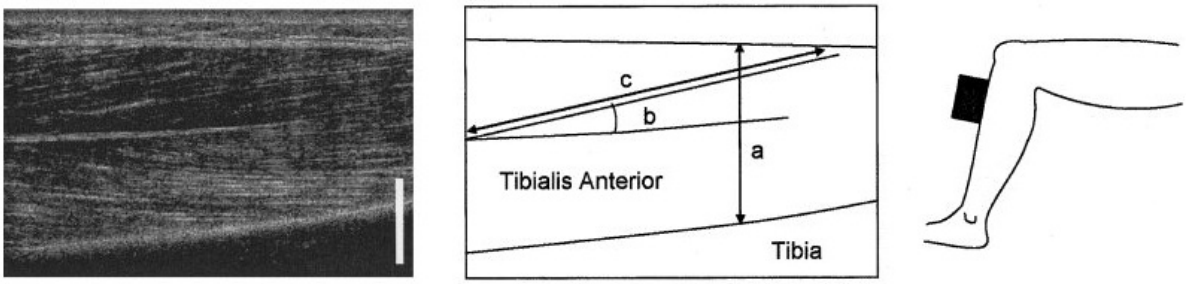

Figure 1.8: The left panel shows an ultrasound image of the TA muscle. The middle panel is an illustration of the main muscle characteristics: (a) thickness, (b) pennation angle and (c) fascicle length. The right panel shows the position and orientation of the ultrasound transducer used during the measurements. All panels show the muscle in relaxed conditions. Figure taken from [38].

By increasing knee flexion, gastrocnemius fibre length decreases and thus its contribution to the ankle torque is reduced, emphasizing the force generated by SOL fibres. This hypothesis has been supported by several studies which report a decreased and constant electromyographic (EMG) activity of gastrocnemius and SOL, respectively, with increasing knee flexion [39, 40, 41, 42, 43].

1.6 Problem statement

The main question that this study aims to address is if it is possible to estimate leg muscles SRS *in vivo* from the ankle joint torque and displacement, using the model previously developed for the wrist [29]. To that end, an haptic manipulator for the ankle will be used to measure torque and ankle displacement and apply fast ramp stretches. Secondly, SRS will be estimated at different knee angles and different pre-stretch torques, to evaluate how gastrocnemius contribution affects this parameter. At last the influence of some parameters, such as muscle architecture, tendon stiffness and muscle moment arm, in SRS will be predicted using a geometrical model.

1.7 Hypothesis

If SRS of the leg muscles can be estimated using the same model used for the wrist joint, we should be able to observe a similar discontinuity in the estimated elastic torque plotted against time and against joint displacement as obtained for the wrist joint (see figure 1.4(b)). Moreover, the estimated model parameters should present low Standard Error Mean (SEM) values and the measured torque should be simulated with high accuracy, presenting a high Variance Accounted For (VAF) value.

SRS is mainly dependent on the number of cross-bridges attached, but it can be influenced by other factors, such as the recruitment of different fibre types, muscles' pennation angle and the stiffness of passive structures. The hypothesis relative to the influence of these parameters on SRS with increasing torque level and increasing knee flexion are summarized in table 1.1.

	Influence in SRS	
Parameter	↑ torque level	↑ knee flexion
Number of cross-bridges	↑	n.a.
Fibre type recruitment	n.s. or ↓	n.s. or ↑
Pennation angle	n.s. or ↓	n.s. or ↓
Passive structures stiffness	↑	n.a.

Table 1.1: Hypothesis for the influence of different parameters (fibre type recruitment, pennation angle and passive structures stiffness) on SRS, measured with increasing torque levels and with increasing knee flexion. ↑ means a positive contribution, ↓ means a negative contribution, n.s. refers to a non significant contribution and, n.a. means not applicable.

If muscle SRS is successfully estimated, it should increase with torque level mainly

due to the increase in the number of cross-bridges attached. However, other parameters are known to contribute to this increase, such as the stiffness of passive structures, which include the Achilles tendon and extracellular connective tissue. With torque level, there is also an increase in leg muscles' pennation angle which is believed to contribute to a reduction in SRS. This contribution might be not significant though [20]. Assuming that type I fibres are recruited before type II fibres [44, 45], a possible increase in the recruitment of type II fibres with torque level could contribute to a lower SRS as well since type II fibres are believed to be less stiff than type I fibres.

Assuming that the number of cross-bridges and the stiffness of passive structures is not affected by the knee angle, these parameters should not influence the estimated SRS at different knee angles. On the other hand, GM and GL's pennation angle increase with knee flexion and could contribute to a lower estimated SRS with the knee flexed. Furthermore, when the knee is flexed, gastrocnemius capacity to produce force is believed to be reduced. Consequently, to generate the same ankle torque with the knee flexed as with the knee extended, more fibres have to be recruited. Assuming that gastrocnemius has a higher content of type II fibres and that these fibres are less stiff than type I fibres, it might be possible to observe differences in SRS with knee angle due to muscle fibre type composition. For lower torques, differences in SRS with knee angle due to fibre type composition are not expected, since at low torques only type I fibres are believed to be recruited. On the other hand, for higher torques SRS is expected to be lower with the knee in extension due to a higher contribution of gastrocnemius type II fibres.

Chapter 2

Method

In this chapter the method used to estimate SRS is described as well as the geometrical model used to predict the contribution of muscle pennation angle, tendon stiffness and muscle moment arm length to muscle stiffness. Furthermore, the statistical analysis performed is also described. In figure 2.1 it is possible to observe a diagram with the main steps of the data processing and statistical analysis performed.

2.1 Instrumentation

In order to estimate muscle SRS, an haptic manipulator was used to amply ramp perturbations to the ankle and measure torque and displacement. The manipulator used was Achilles (MOOG FCS Inc., Nieuw Vennep, The Netherlands), which has a single degree of freedom about the sagittal plane allowing plantarflexion/dorsiflexion of the foot. The manipulator is composed of a motor, equipped with an angular encoder to measure angular displacement, and a footplate, equipped with strain gauges to measure the exerted torque on the footplate. Data were collected with a sampling frequency of 2048 Hz. The experimental set-up is shown in figure 2.2.

Muscle activity of the leg muscles was assessed using an electromyographic (EMG) system (Bagnoli 8 system, Delsys, Boston). Before the electrodes placement, the skin was first cleaned with a skin preparation gel (SkinPure, Nihon Kodhen) and after with alcohol 70% with 10% isopropylalcohol. The electrodes were positioned on the TA, SOL, GM and GM muscles according to the SENIAM guidelines [46], except the reference electrode, which was placed behind the knee since the recommended location, the ankle, was not stable during the experiment. To improve the contact between the reference electrode and the skin, a conductive gel (Medi-trace) was used. The EMG system and Achilles were synchronized via an AD-converter (National Instruments USB-6221). Both the AD-converter and Achilles were connected to the laptop where

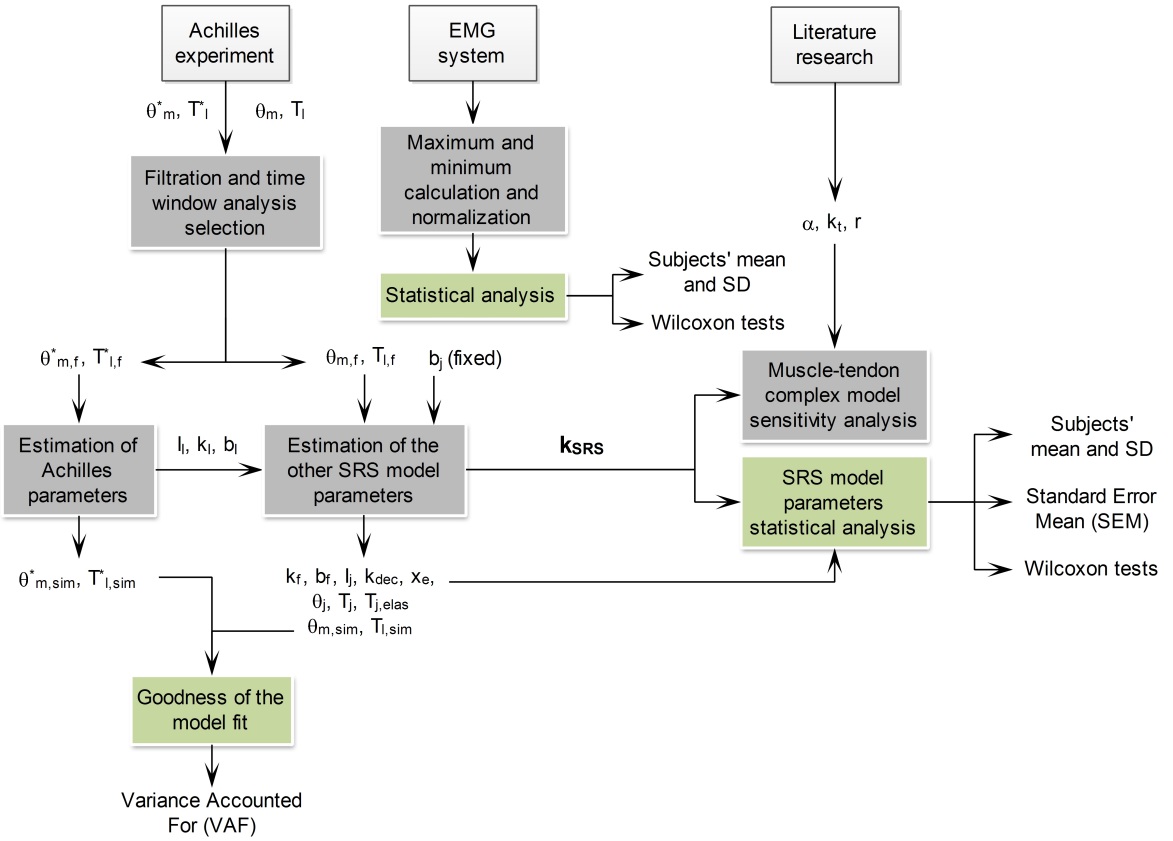

Figure 2.1: Data flow of the experiment. During the SRS experiment, data were collected with the Achilles manipulator and the electromyographic (EMG) system. The measured torque (T_l^*) and displacement (θ_m^*) obtained without a subject, were filtered ($T_{l,f}^*$, $\theta_{m,f}^*$) and, using a time window analysis of 55 ms, the Achilles parameters were estimated (I_l, b_l, k_l). The measured torque (T_l) and displacement (θ_m) obtained with the subjects were also filtered ($T_{l,f}$, $\theta_{m,f}$). Using the same time window analysis, and the Achilles parameters previously estimated, the other parameters of the SRS model were estimated (k_f,b_f,I_j,k_{dec},x_e and k_{SRS}). Joint damping (k_j) was fixed as being 1×10^{-2}. The goodness of the model fits was evaluated through the Variance Accounted For (VAF) values, calculated from the simulated torque relative to measurements done with ($T_{l,sim}$) and without a subject ($T_{l,sim}^*$) attached to the manipulator. The main parameter of interest was k_{SRS}. The Wilcoxon test was used to evaluate if there were significant differences in k_{SRS} measured at different torque levels and different knee angles. Moreover, the estimated parameters were analysed by calculating the subjects' mean, standard deviation (SD) and standard error mean (SEM). Furthermore, k_{SRS} values were used as input in the muscle-tendon complex (MTC) model developed. The other variables of the model were estimated from the literature. Regarding the EMG data of each muscle (SOL, GM, GL and TA) collected during the SRS experiment, the maximum and minimum were calculated for each subject. The mean value of each muscle EMG activity, during the first 500 ms before the ramp perturbation was applied, was calculated and normalized for each subject. Significant differences in the mean EMG values with torque level and knee angle were analysed using the Wilcoxon test. In general, grey blocks refer to steps related to data processing and green blocks to statistical analysis.

the data were being stored and which displayed the visual feedback to the subject during the experiment. EMG data were collected using a sampling frequency of 1500 Hz.

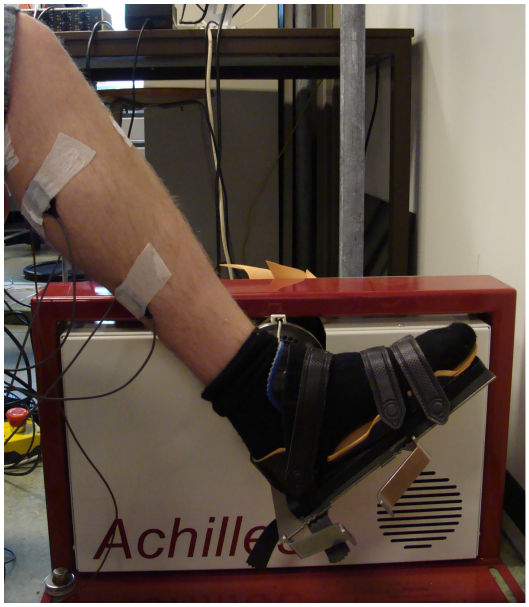

Figure 2.2: Set-up of the ankle manipulator. The foot was tightly strapped to the footplate and a support was used under the main velcro strap to minimize the foot movement in other directions than plantarflexion.

2.2 Experimental procedure

During the experiment, the subject was sat on a chair with the left foot attached to the ankle manipulator by velcro straps (see figures 2.2 and 2.4). The subject was asked to generate a determined torque in the plantarflexion direction and, when the torque was maintained for 0.5 seconds, allowing a deviation of 1%, a ramp perturbation was applied. The ramp caused the foot rotation in the dorsiflexion direction, resulting in a stretch of the TS muscles. As previously mentioned, the subjects were guided by visual feedback, represented in figure 2.3, where they could observe the torque being generated and the target torque. The ramp perturbation had an amplitude of 0.15 rad, corresponding to approximately 8.6°, a duration of 167 ms and a maximal angular velocity of approximately 2 rad/s. Each subject had to generate four torque levels (0, 5, 10, 15 and 20 Nm) and three repetitions were performed for each torque level. At 0 Nm, the subjects were instructed to relax and the ramp was automatically applied. For each subject, the measurements were performed with the leg in two different positions: with the knee extended, corresponding to 180°, and with the knee flexed at 90°, as shown in figure 2.4. The leg position could be adjusted by moving the chair forward or backwards. The order of torque levels was aleatory as well as the order of the knee position to be used.

At both knee positions, the initial position of the foot was adjusted, by eye, to 90°, corresponding to the angle between the sole foot and the tibia, and the trunk was

slightly extended. All subjects performed the experiment with the left leg due to the configuration of the manipulator. The foot position was also adjusted by eye so that the foot plantarflexion-dorsiflexion axis was aligned with the motor axis. To minimize movements in other planes and improve the contact between the foot and the footplate, the foot was tightly strapped and a support was used under one of the velcro straps, as it is possible to observe in figure 2.2. Before starting the experiment, the EMG signals were observed in real time and the electrodes were repositioned if necessary. In total, ten healthy male subjects, aged 24-51 years, were measured. The study population was exclusively male since differences in SRS between genders were previously found for the wrist muscles [30]. Two of the subjects were measured in two different days to test the repeatability of the SRS estimation method, which provides information about the method's reliability.

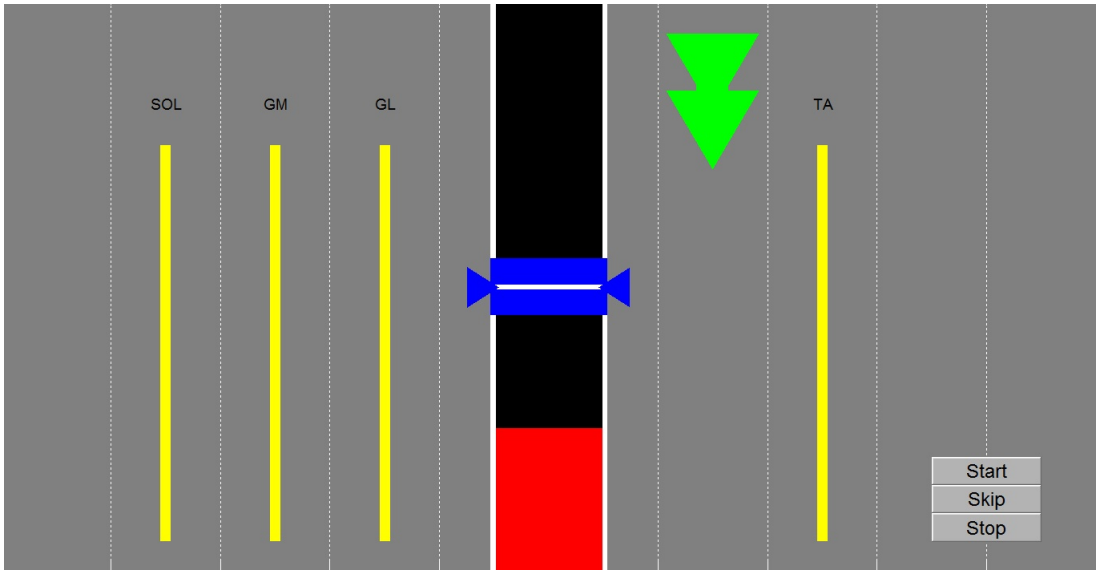

Figure 2.3: Visual feedback provided during the SRS measurements. The ankle torque was visualized by a moving vertical red bar that emerges from the bottom. The green arrow indicates the direction of the torque to be applied (plantarflexion). Target torque is indicated by the blue area (±1% of torque level). SOL, GM, GL and TA activity were displayed by vertical yellow bars whose height was proportional to the standard deviation (SD) of the EMG signal divided by the maximum signal of the corresponding muscles.

2.3 Data processing and statistical analysis

SRS model parameters were estimated using a non-linear least squares method to minimize the error between the measured (T_l) and the simulated torque ($T_{l,sim}$) defined as:

$$T_{l,sim} = (\dot{\theta}_m - \dot{\theta}_l)b_l + (\theta_m - \theta_l)k_l \tag{2.1}$$

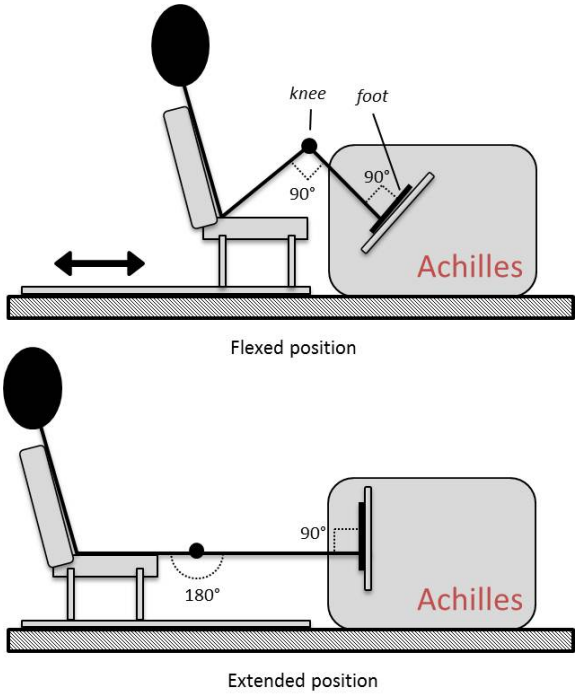

Figure 2.4: Illustration of the leg positions used during the SRS experiment. Subjects performed the experiment with the leg extended, corresponding to a knee angle of 180°, and with the leg flexed, corresponding to a knee angle of 90°. The initial foot position was always the neutral position, which corresponds to an angle of 90° between the tibia and the sole foot. Ankle and knee angles were adjusted by eye while the subject was being attached to the manipulator.

The initial measured torque and the initial measured angular displacement were subtracted before the analysis since the model describes only changes with respect to steady state. The manipulator's parameters (I_l, k_l and b_l) were estimated first from the measured torque (T_l) and the measured angular displacement (θ_m) when applying a ramp perturbation without a subject attached to the manipulator. A reduced version of the SRS model, only with subsystem I, was used for this purpose (see figure 1.5). These parameters were fixed for the analysis of the subjects. Joint damping (b_j) was also fixed with a low value of 1×10^{-2}, since the joint should demonstrate a low damping due to the initial high muscle stiffness, corresponding to SRS. Therefore, for each subject a total of 6 parameters were estimated (k_f, b_f, I_j, k_{SRS}, k_{dec} and x_e) for each torque level and for both knee angles at which measurements were done.

Before calculating the SRS model parameters, T_l and θ_m were filtered with a 3^{rd} order Butterworth low-pass filter with a cut-off frequency of 50 Hz. In addiction, a time window width of 55 ms was used for the analysis to avoid the influence of reflexes, which appeared approximately 60 ms after the ramp perturbation, as shown in the raw EMG signals (see figure D.1 in appendix D).

The goodness of the model fit was evaluated through the Variance Accounted For (VAF) values:

$$VAF = 1 - \frac{\sum_{i=1}^{n}(T_{l,i} - T_{l,sim,i})^2}{\sum_{i=1}^{n}(T_{l,i})^2} \tag{2.2}$$

where i indicates the time sample, n=113 is the number of data points used for the parameter estimation and $T_{l,i}$ and $T_{l,sim,i}$ are the measured and the simulated torques at the i$_t h$ time sample, respectively.

Parameter's reliability was indicated by the Standard Error of the Mean (SEM):

$$SEM = \sqrt{\frac{1}{n} I (J^T J)^{-1} \sum_{i=1}^{n}(E_i)^2} \tag{2.3}$$

with $E_i = T_{l,i} - T_{l,sim,i}$ the error, J is the Jacobian ($n \times n_p$ vector of first derivatives of the error of each parameter, with $n_p = 6$ the number of parameters) and I the identity matrix. The SEM equals the deviation of the parameter to its theoretical value at the minimal (optimal) error.

Some repetitions were excluded from the analysis due to errors during the model simulations or because the data were corrupted, due to bad contact between the foot and the manipulator, clearly observed in the measured torque traces. For one subject, regarding measurements performed at two torque levels with the knee extended, there were only two repetitions available because the subject was having difficulty in finishing the task. One subject was excluded from the analysis at zero torque level because the initial measured torque was relatively high (close to 5 Nm), which means that the subject was not relaxed as instructed.

The model parameters were averaged over trials and subjects as follows:

$$p_{i,j} = \sum_{m=1}^{n_m} \sum_{k=1}^{n_k} p_{i,j,k,m} / (n_m n_k) \tag{2.4}$$

where k refers to the trial order, being n_k the number of trials available for a certain torque level, m refers to the subject order, being n_m the number of subjects, and i refers to the parameter order, being n_i the number of parameters.

The SEM values were normalized with respect to the corresponding parameter value and averaged over subjects and trials:

$$SEM_{i,j} = \sum_{m=1}^{n_m} \sum_{k=1}^{n_k} \left(\frac{SEM_{i,j,k,m}}{p_{i,j,k,m}} \right) / (n_m n_k)) \tag{2.5}$$

Furthermore, inter-trial standard deviations (ITSTD) of the estimated parameters were calculated for each subject, normalized with respect to the parameter's mean and

averaged over subjects:

$$ITSTD_{i,j} = \sum_{m=1}^{n_m} \sum_{k=1}^{n_k} (p_{i,j,k,m} - \overline{p}_{i,j,m})^2 / (\overline{p}_{i,j,m}(n_k - 1)n_m) \tag{2.6}$$

where

$$\overline{p}_{i,j,m} = \sum_{m=1}^{n_m} p_{i,j,k,m}/n_m \tag{2.7}$$

The raw EMG signals of the four muscles (GM, GL, SOL and TA) were de-trended, rectified and filtered with a 3^{rd} order Butterworth low-pass filter with a cut-off frequency of 20 Hz [47]. For each subject and each muscle, the maximum (EMG_{max}) and minimum (EMG_{min}) values were calculated over all trials. Furthermore, using a time window width of 500 ms prior to the ramp perturbation, the mean EMG ($\overline{EMG}$) values of each muscle were calculated for each torque level, averaged over trials and normalized for each subject, according to the maximum (1) and minimum (0) levels previously calculated. The mean normalized EMG ($\overline{EMG}_n$) of each subject was calculated as follows:

$$\overline{EMG}_n = \frac{\overline{EMG} - EMG_{min}}{EMG_{max} - EMG_{min}} \tag{2.8}$$

A time window width of 500 ms was chosen since it was the minimum time required to trigger the ramp perturbation while generating a determined stable torque level. One subject was excluded from the EMG analysis since the raw signals contained a lot of noise, probably due to a bad contact between the electrodes and the skin. For the 0 Nm torque level, a time window of 200 ms had to be used because the recordings were shorter. For all torque levels, the first second of the EMG recordings was excluded, since it is highly contaminated by noise, except for the 0 Nm torque level due to the duration of the recordings, as previously mentioned.

The distribution of the subjects' mean k_{SRS} and of the mean normalized EMG of each muscle ($\overline{EMG}_n$), for each torque level and each knee angle, was analysed using histograms. Since the distributions weren't either normal nor symmetric, the Wilcoxon test for paired samples was used to test the following null hypothesis:

- there is no significant increase in the mean k_{SRS} with torque level (for each knee angle);
- there is no significant difference between the mean k_{SRS} measured at different knee angles (considering a certain torque level);
- there is no significant increase in the $\overline{EMG}_n$ of the leg muscles with torque level;

- there is no significant difference between the $\overline{EMG}_n$ of the leg muscles measured at different knee angles (considering a certain torque level);
- there is no significant difference between the mean k_{SRS} of the two subjects measured at different days.

The dependent variable was assumed to be the torque level or the knee angle and the independent variable was the mean k_{SRS} or the muscle $\overline{EMG}_n$. A significance level of 5% was used, which means that if the p-value (p) of a determined test is lower than 0.05 we may reject the null hypothesis.

2.4 Muscle-tendon complex model

In the SRS model developed by Eesbeek et. al [29] no attempt was made to discriminate between muscle and tendon stiffness. Therefore, when estimating k_{SRS}, we assume that ankle stiffness mainly reflects muscle stiffness, and the contribution of the tendon and muscles' pennation angle are neglected. For this reason, a geometrical model was developed where ankle stiffness (k_j) results from the stiffness of the muscle and tendon, which are represented by two non-linear springs connected in series, characterized by a stiffness k_m and k_t respectively, with a certain angle α between each other, representing muscle pennation angle. This model is illustrated in figure 2.5. The model represents only one muscle-tendon complex (MTC), since the method used to estimate joint stiffness previously described doesn't allow the discrimination of different muscles that contribute to joint stiffness.

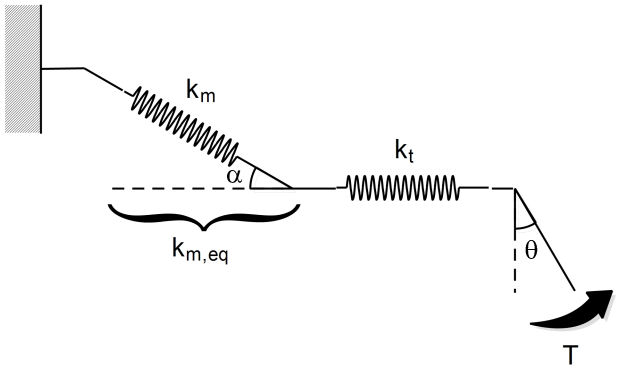

Figure 2.5: Muscle-tendon complex model of the leg used to study the contribution of pennation angle and tendon stiffness to joint stiffness. The muscle and the tendon are modelled as two non-linear springs connected in series with stiffness k_m and k_t respectively. The angle between the springs corresponds to muscle pennation angle (α) and it depends both on torque level (T) and ankle angle (θ).

Muscle effective stiffness ($k_{m,eq}$) depends on pennation angle (α) as follows:

$$k_{m,eq} = k_m \cos\alpha \tag{2.9}$$

Therefore, according to this model, ankle stiffness (k_j), i.e. the resistance of the ankle to movement, is related to $k_{m,eq}$ and k_t by the following equation:

$$k_j = \frac{k_{m,eq} k_t}{k_{m,eq} + k_t} r^2 \tag{2.10}$$

where r is the moment arm length, which is the distance between the joint rotation centre and the muscle's line of action.

The input parameters of the MTC model are muscle pennation angle (α), joint stiffness (k_j), tendon stiffness (k_t) and moment arm length (r). These parameters were assumed to be dependent on the torque being produced at the ankle level (T). The relationships between the parameters and torque level were derived from literature and are described in table 2.1. The output parameter of the model is muscle stiffness (k_m), the parameter that we are effectively trying to estimate with the SRS model. k_m is related to $k_{m,eq}$ by equation 2.9 and it can be calculated as:

$$k_m = \frac{-k_j k_t}{\cos\alpha(k_j - k_t r^2)} \tag{2.11}$$

As previously mentioned, the relationships between the input parameters and T were derived from literature, considering measurements performed with the ankle in the neutral position ($\theta = 90°$), since θ influences the value of these parameters and it is the initial foot position used in the SRS experiment. k_j was assumed to correspond to muscle SRS (k_{SRS}) and to vary linearly with T. Its values were extrapolated from the results previously obtained with the SRS model. The relationship between k_t and T was derived from the Achilles stiffness values reported by Maganaris et. al [48] which were related to different percentages of maximum voluntary contraction (MVC) torque. The relationship between r and T was assumed to be linear and derived from the values reported, at rest and during MVC, by Maganaris et. al [48, 49].

Regarding α, it depends not only on T but also on the knee angle at which the measurements are performed, considering muscles that are both attached to the ankle and to the knee joints, such as GM and GL. The largest change in leg muscles' α with knee angle was found for GM, which decreases by 38%-33%, at rest and during MVC respectively, when the knee angle changes from 90° to 180° (fully extended) [33]. The relationship between α and T was derived from a study of Maganaris et. al [50], where a regression equation of α in function of % MVC was available for GM, considering measurements done with the knee flexed at 90°. However, since the mean MVC torque was not reported in this study, the value reported by [36] was used to derive the α-T

relationship.

Parameter	Range (rest-MVC)	MVC moment (Nm)	Parameter-T relationship	Ref.
k_t (N/m)	4.8×10^4-1.5×10^5	162	$k_t = -3.0 \times T^2 + 1.2 \times 10^3 \times T + 2.8 \times 10^4$	[48]
r (m)	4.9×10^{-2}-6.3×10^{-2}	162	$r = 1.0 \times 10^{-4} \times T + 4.9 \times 10^{-2}$	[49, 48]
α (°)	22.9-42.0	110*	$\alpha = 2.0\times10^{-3}\times T^2 - 4.8\times10^{-2}\times T + 2.3\times10^1$	[50]

Table 2.1: Input parameters of the MTC model and the equations used to describe their relationship with torque level (T). * - This MVC moment value was estimated from the values reported by Maganaris [36].

To analyse how k_m changes with these parameters, a sensitivity analysis was performed, which consists in changing a single input parameter of the model (k_t, r or α), while maintaining the others constant. The percentage variation in the input parameters was also derived from literature, in order to assume reliable variations. Regarding k_t variation, Maganaris et. al 2002 [48] report a standard deviation of k_t between 12000 Nm and 28000 Nm, regarding measurements done at rest and during MVC, respectively. A variation of this magnitude corresponds to a change between 37% to 19%, respectively. In the same study, the authors report a standard deviation for r of 4 mm. A decrease in r of only 4 mm corresponds to a decrease between 8% and 7% at rest and during MVC, respectively. The variation of α considered was between 38% and 33%, from rest to MVC, the largest change in leg muscles' α reported, considering either measurements done at different torque levels and different knee angles, as mentioned above. In general, the parameters' variation was higher at rest and it was assumed to decrease linear until MVC torque. The change in k_m (Δk_m) that results from a change in the one of the input parameters (Δp) was calculated as follows, for a determined torque level:

$$\Delta k_m = \frac{k_{m,f} - k_{m,i}}{k_{m,i}} \tag{2.12}$$

where $k_{m,i}$ is the muscle stiffness estimated with the input parameters values presented in table 2.1, i.e. without any change, and $k_{m,f}$ is the muscle stiffness estimated with a change in one of the parameters ($p_f = p_i - \Delta p$) maintaining the values of the other parameters constant.

All data were processed in Matlab® R2011b and the statistical tests were performed in SPSS® version 19.

Chapter 3

Results

In this chapter, the data collected with Achilles, the SRS model simulations and the statistical analysis results are presented. The results of the sensitivity analysis of the MTC model are also shown here.

3.1 SRS model parameters estimation

3.1.1 Achilles parameters (subsystem I)

As described in the Method section, the Achilles dynamics were first estimated from the three measurements performed without a subject attached to the manipulator. This was done by using a reduced version of the SRS model, i.e. only containing the subsystem I (see figure 1.5). In figure 3.1.A and 3.1.B it is possible to observe the raw data, obtained with Achilles, more specifically the measured displacement (θ_m) and the measured torque (T_l) during one the trials. A 55 ms time window was used for the optimization and an example of the simulated displacement ($\theta_{m,sim}$) and simulated torque ($T_{l,m}$) can be observed in figure 3.1.C and 3.1.D, respectively. The estimated parameters' values and respective SEM, for each repetition, are presented in table 3.1 as well as the VAF of the model fits and the measured initial torque before the ramp perturbation (T_0).

The manipulator's inertia (I_l) was the most consistent estimated parameter over repetitions, presenting a mean $\pm$ SEM value of 0.0231 $\pm$ 0.0147 km m^2. The other parameters (b_l and k_l) presented a high discrepancy over the different repetitions, even though they were characterized by low SEM values. Despite the great similarity between the T_l and θ_m obtained in the three repetitions, b_l ranged from 0.7-44 Nm s/rad and k_l varied between 2082-17050 Nm/rad (see table 3.1).

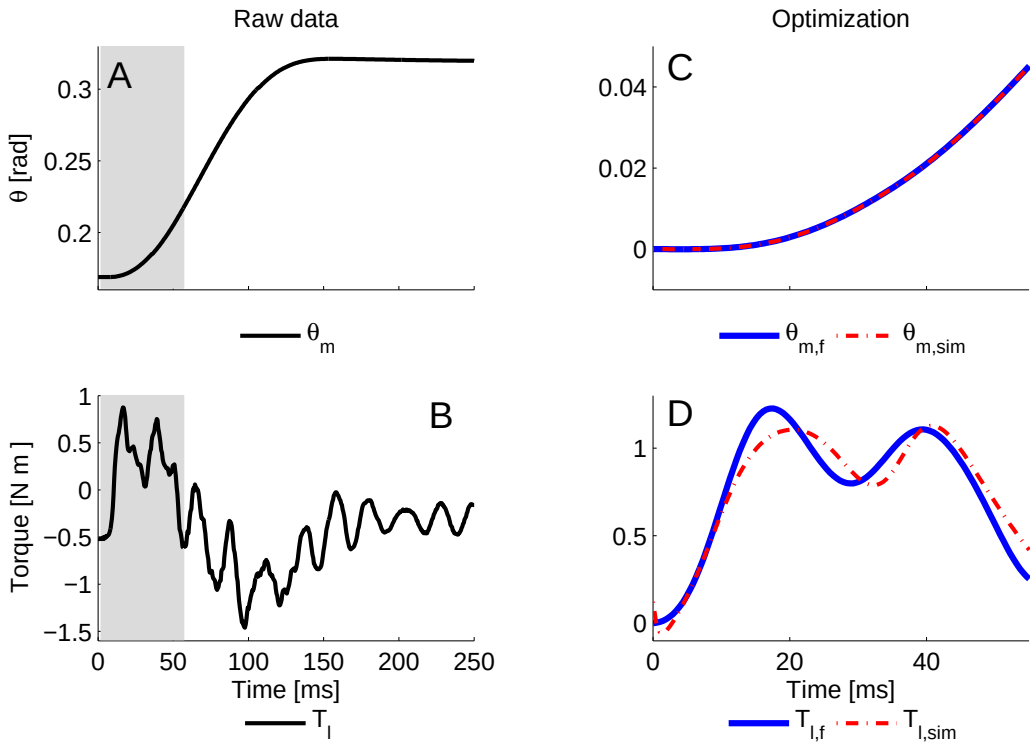

Figure 3.1: Example of the raw data (A,B) obtained with Achilles when applying a ramp perturbation without a subject attached to the manipulator and corresponding output of the SRS model simulation (C,D). (A) Measured angular displacement (θ_m) and (B) measured torque (T_l), both limited by a grey shadow that corresponds to the 55 ms time window used for optimization. (C) Filtered measured displacement used for optimization ($\theta_{m,f}$) and simulated measured displacement ($\theta_{m,sim}$). (D) Filtered measured torque used for optimization ($T_{l,f}$) and simulated measured torque ($T_{l,sim}$).

Parameter value ± SEM	Repetition 1	Repetition 2	Repetition 3
I_l (kg m^2)	0.0232 ± 0.0142	0.0239 ± 0.0154	0.0222 ± 0.0144
b_l (Nm s/rad)	5.4678 ± 0.3543	44.9355 ± 0.7474	0.6846 ± 0.2354
k_l (Nm/rad)	4322.7 ± 0.1587	17050 ± 0.5575	2082.4 ± 0.0274
VAF (%)	97.8033	98.6154	97.7893
T_0 (Nm)	-0.5813	-0.5772	-0.5638

Table 3.1: Estimated Achilles' inertia (I_l), damping (b_l) and stiffness (k_l). These parameters were estimated from the three measurements performed without a subject attached to the manipulator. It is also possible to observe the VAF of the model fit and the initial measured torque (T_0) regarding each repetition.

3.1.2 Interface and joint parameters (subsystems II and III)

For the subjects' analysis, the parameters of the manipulator were fixed as being the one's from the second repetition, whose model simulation had the highest VAF (see table 3.1). To increase the VAF of the subjects' simulations, I_l and b_l were adjusted and fixed as being 0.00239 kg m^2 and 0.449355 Nm s/rad, respectively. Regarding k_l,

the original value of 17050 Nm/rad was used. These values are more similar to those obtained for the wrist manipulator [29], except k_l which is approximately 100 times higher. b_j was also fixed as being 1×10^{-2} Nm s/rad, a low value since no joint damping is expected due to the initial high muscle stiffness. For the wrist, a relatively lower value was used (1×10^{-5}) [29].

In appendix B, it is possible to observe the raw data obtained with Achilles, at different torque levels, relative to measurements done with subjects. In table B.1, we can observe the measured torques (T_l) for all subjects, used for the simulations, and figure B.1 shows the measured torques, averaged over subjects, during a longer time interval, for both knee angles. As we can observe in these figures, there are no big discrepancies in the measured torques between subjects and no visible significant differences between measurements done at different knee angles. Figure B.2 shows an example of the commanded, measured and filtered displacement, velocity and acceleration for one subject, at two different pre-stretch torque levels. The commanded displacement corresponds to the modelled ramp perturbation that was applied to the subject. As we can see, there are some artefacts in the measured velocity and acceleration but these were successfully filtered. For torques higher than 0 Nm, it is possible to observe that the manipulator could not reach the maximum velocity of the modelled ramp. This means that the actual ramp applied to the subject was slightly less steep than the modelled ramp. Similar results were observed when subjects performed the experiment with the knee extended.

In figures 3.2.A and 3.2.B, it is possible to observe the measured angular displacement (θ_m) and the measured torque (T_l) respectively, obtained with Achilles during a trial characterized by a pre-stretch torque level of 10 Nm. In figures 3.2.C and 3.2.D, the outcome simulations of the SRS model are presented: the simulated measured displacement ($\theta_{m,sim}$), the simulated joint displacement (θ_j), the simulated measured torque ($T_{l,sim}$), the simulated joint torque (T_j) and the simulated elastic part of the joint torque ($T_{j,elas}$). $\theta_{m,f}$ and $T_{l,f}$ are the filtered measured angular displacement and torque respectively, which were used as input in the model simulations.

In figures 3.3.A and 3.3.B, it is possible to see an example of the simulated elastic joint torque ($T_{j,elas}$), obtained for the different torque levels, plotted against time (t) and against joint angular displacement (θ_j), respectively. k_{SRS}, which is plotted against torque level in figure 3.3.C, corresponds to the slope of the relationship between $T_{j,elas}$ and θ_j before the discontinuity observed (see figure 3.3.B). The joint position (θ_j) at which this transition occurs corresponds to the elastic limit (x_e). It is important to point out that this discontinuity associated with k_{SRS} was not clear in all repetitions.

The estimated SRS model parameters and the corresponding SEM, averaged over

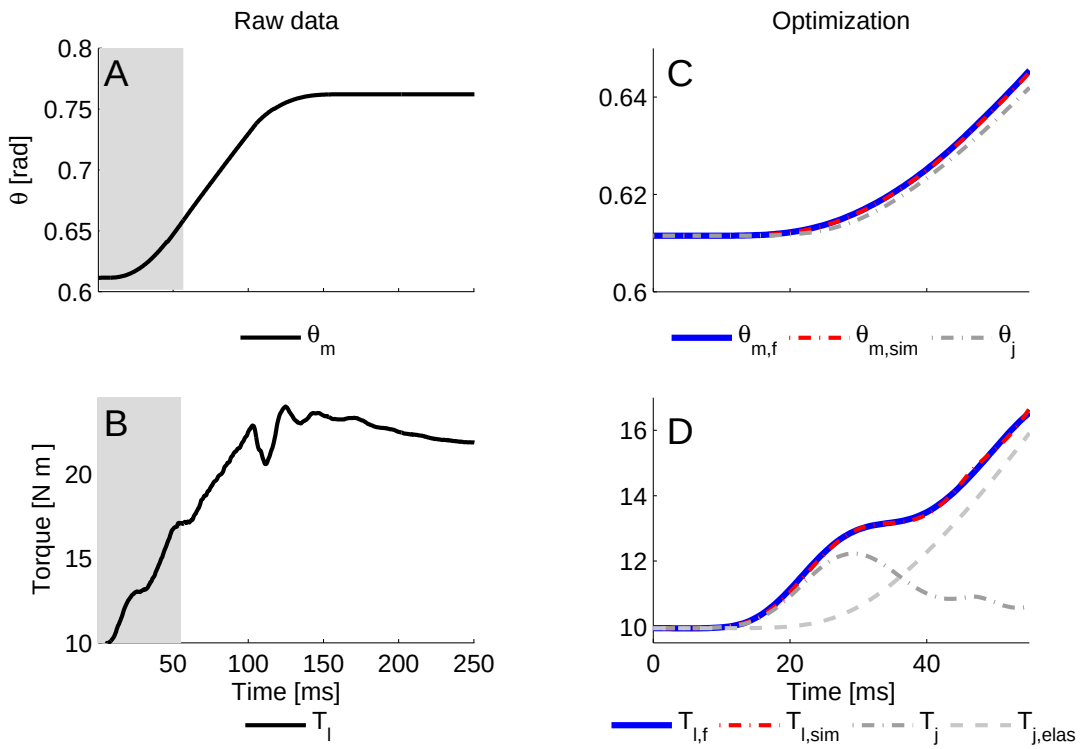

Figure 3.2: Example of the raw data (A,B) obtained with Achilles after applying a ramp perturbation, when a subject is generating a torque level of 10 Nm, and the respective output of the SRS model simulation (C,D). (A) Measured angular displacement (θ_m) and (B) measured torque (T_l), both limited by a grey shadow that corresponds to the 55 ms time window used for optimization. (C) Filtered measured displacement used for optimization ($\theta_{m,f}$), simulated measured displacement ($\theta_{m,sim}$) and simulated joint displacement (θ_j). (D) Filtered measured torque used for optimization ($T_{l,f}$), simulated measured torque ($T_{l,sim}$), simulated joint torque (T_j) and simulated elastic part of the joint torque ($T_{j,elas}$).

repetitions and subjects, are presented in table C.1, in appendix C, as well as the mean VAF and mean measured T_0 for each torque level and for each knee angle. For all torque levels, the simulations had high VAF values and most of the parameters show a low SEM, except k_{dec} and x_e. Moreover, in figure 3.4 it is possible to observe the mean ITSTD of the estimated parameters, which is considerably high for all parameters, excluding I_j and k_{SRS}, irrespective the torque level considered. Figure C.1, in appendix C, shows the mean ITSTD of the parameters' SEM.

The main parameter of interest of the SRS model was k_{SRS}. In figure 3.5, we can see its mean values and corresponding SD for each torque level, at each knee angle. Comparing the mean k_{SRS} estimated from the measurements done with the knee flexed and with the knee extended, there was a difference of approximately 6%, -12%, -7%, 1% and -12% at 0, 5, 10, 15 and 20 Nm, respectively. According to the Wilcoxon test results, these differences were found to be not significant ($0.144<p<0.859$). Regarding the increase in k_{SRS} with torque level, it was significant from 0 to 5 Nm ($p=0.008$,$p=0.008$),

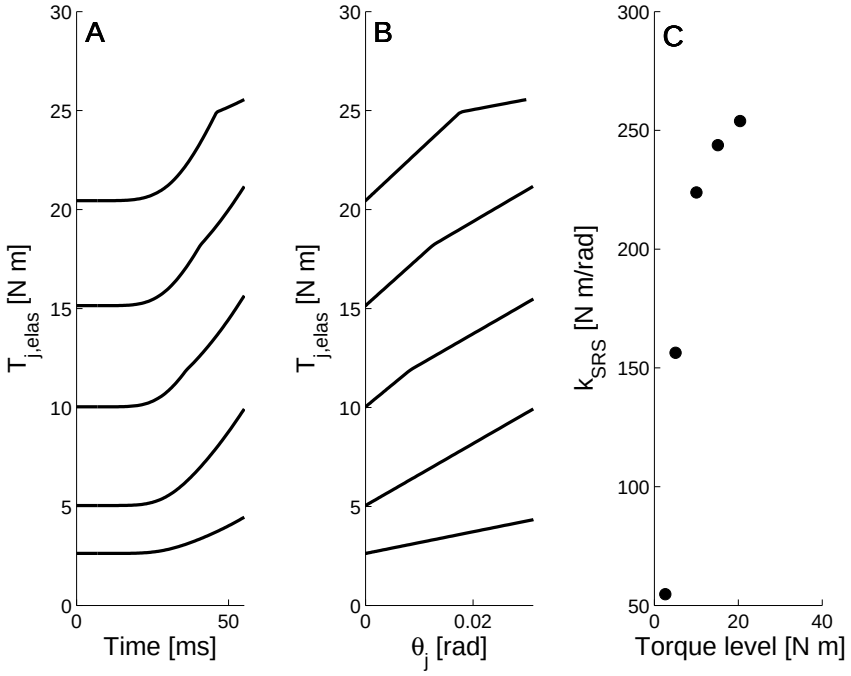

Figure 3.3: Example of the simulated $T_{j,elas}$ as function of (A) time and (B) joint displacement (θ_j), concerning different torque levels. It is possible to observe a transition point in the $T_{j,elas}$-θ_j traces which corresponds to the joint elastic limit (x_e). This discontinuous derivative is believed to result from the transition between an initial high joint stiffness, which corresponds to muscle SRS, followed by a decline. (C) k_{SRS} plotted against pre-stretch torque level.

from 5 to 10 Nm (p=0.013,p=0.009) and from 10 to 15 Nm (p=0.022,p=0.007), relative to measurements done with the knee flexed at 90° and extended, respectively. From 15 to 20 Nm, the increase in k_{SRS} was not statistically significant (p=0.059,p=0.646). These results are illustrated in figure 3.5 as well.

3.2 EMG data

In figure D.1, in appendix D, it is possible to observe an example of the raw, rectified and filtered EMG signals of the different leg muscles, obtained during the SRS experiment performed at a torque level of 5 Nm. The appearance of the stretch reflex of the TS muscles is clear in this figure and it occurs approximately 60 ms after the beginning of the ramp perturbation. In addiction, the reflexes of the TS muscles seem to be synchronized. The mean normalized EMG ($\overline{EMG}_n$) of SOL, GM, GL and TA muscles, prior to the ramp perturbation, are shown in figure 3.6, for all torque levels at both knee angles.

According to the Wilcoxon test results, the only significant differences found between the $\overline{EMG}_n$ measured at different knee angles was for the GM muscle at a torque level of 5 Nm (p=0.037). Regarding the increase in the $\overline{EMG}_n$ with torque level, it

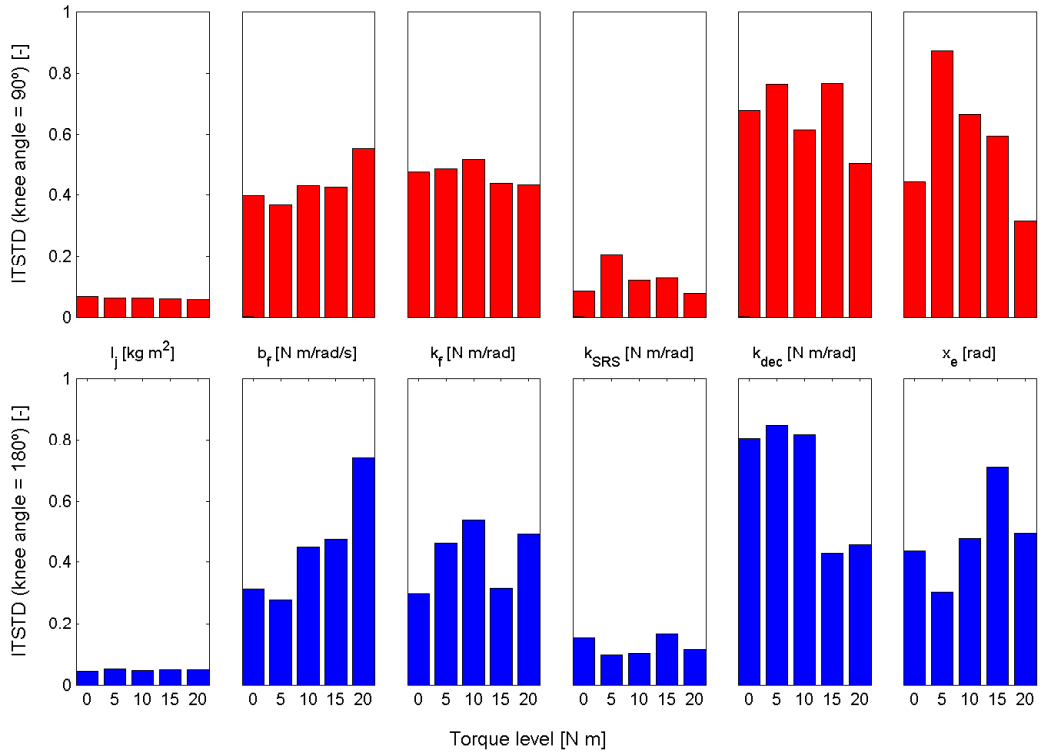

Figure 3.4: Mean normalized inter-trial standard deviations (ITSTD) of the estimated parameters regarding subjects' analysis, for the different torque levels and for both knee angles at which measurements were performed, 90° (in red) and 180° (in blue).

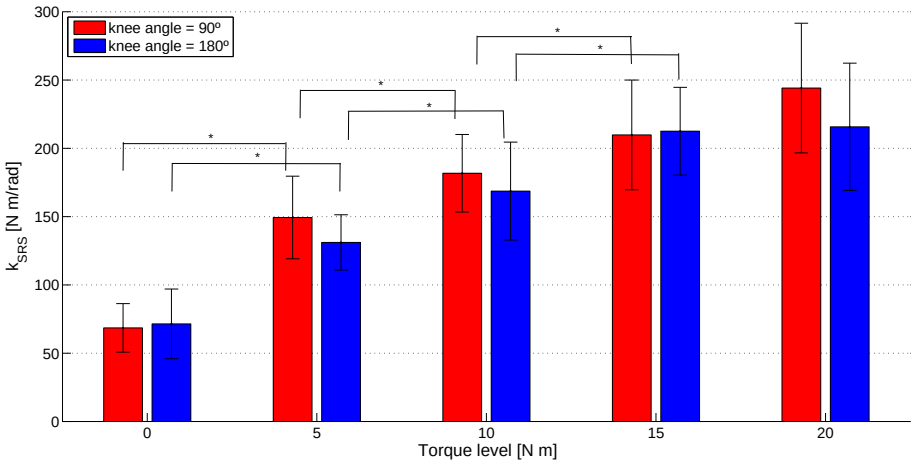

Figure 3.5: Mean k_{SRS} for the different torque levels for both knee angles at which measurements were performed, 90° (in red) and 180° (in blue). The error bars represent the mean SD. * denotes a significant increase ($p<0.05$) in k_{SRS} with torque level.

was statistically significant: for the SOL muscle from 15 Nm to 20 Nm with the knee flexed ($p=0.017$), for the GM muscle from 10 Nm to 15 Nm ($p=0.022$) and from 15 Nm to 20 Nm ($p=0.022$) with the knee extended and, for the GL muscle from 15 Nm to 20 Nm with the knee flexed ($p=0.017$) and from 5 Nm to 10 Nm with the knee extended

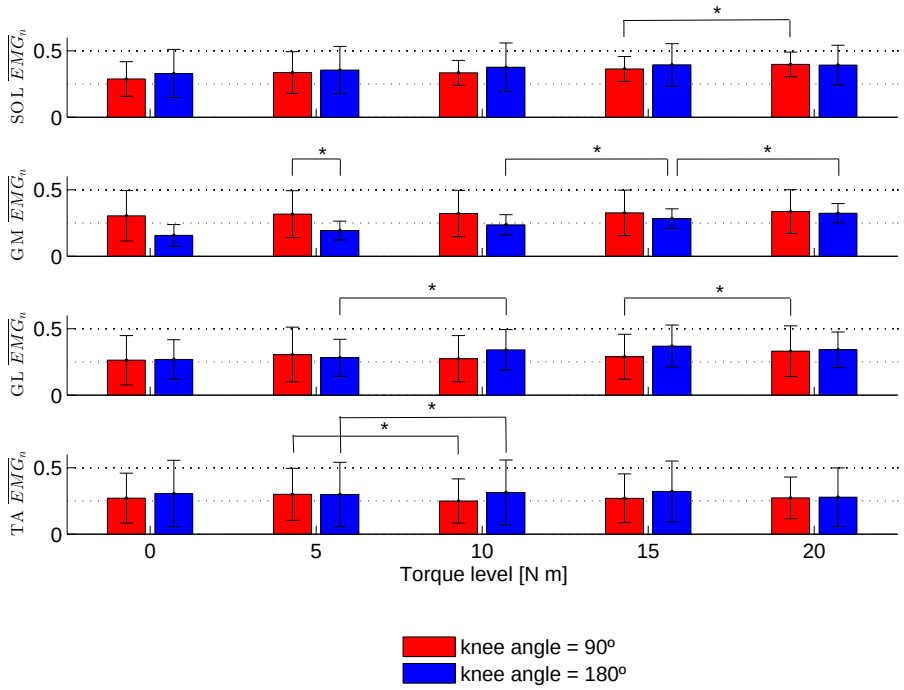

Figure 3.6: Mean normalized EMG ($\overline{EMG}_n$) of the main plantar flexors (SOL, GM and GL) and the main dorsiflexor (TA), for the different torque levels and for the measurements performed with the knee extended, corresponding to 180° (in blue), and with the knee flexed at 90° (in red). * denotes a significant difference ($p<0.05$) between the $\overline{EMG}_n$ of a determined muscle measured at different knee angles or at different torque levels.

($p=0.005$). Regarding the TA muscle, there is a significant decrease in the $\overline{EMG}_n$ from 5 Nm to 10 Nm, with the knee flexed ($p=0.047$), and a significant increase at the same torque level with the knee extended ($p=0.005$). These results are illustrated in figure 3.6. The values relative to the zero torque level (0 Nm) were not included in the statistical analysis because the data used to calculate the $\overline{EMG}_n$, at this torque level, is likely to be corrupted.

3.3 Repeatability analysis

In figure 3.7, it is possible to observe the mean estimated parameters of two subjects, measured on different days. The most consistent parameter seems to be joint inertia (I_j). No significant differences were found between the mean k_{SRS} estimated from measurements done at different days ($0.180<p<0.655$). However, k_{SRS} is relatively higher on the second day, concerning measurements performed with the knee extended (180°). Regarding the other parameters (b_f, k_f, k_{dec} and x_e), their mean value and SD is noticeably lower on the second day comparing to the first day, in particular at higher torque levels.

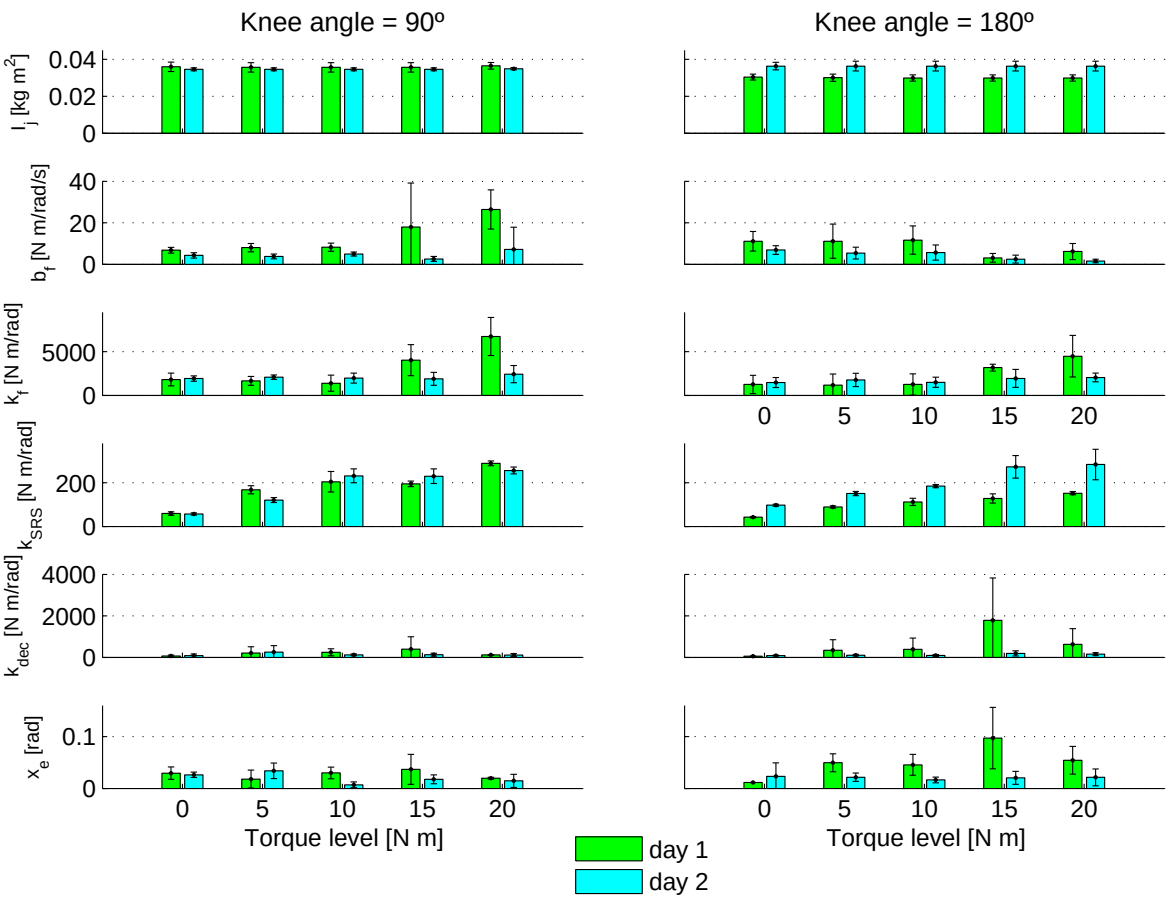

Figure 3.7: Mean values of the estimated SRS model parameters of two subjects, measured on two different days, with the knee flexed at 90° and extended (180°).

3.4 Muscle-tendon complex model - sensitivity analysis

According to the results of the sensitivity analysis of the MTC model, presented in table 3.2, in general muscle stiffness (k_f) decreases with lower tendon stiffness (k_t), lower muscle moment arm length (r) and lower muscle pennation angle (α).

Regarding a change in k_t ranging from 37% to 19%, it results in a maximal decrease of approximately 71.6% in k_m at rest, i.e. at a torque level of 0 Nm. Considering a decrease in r of only 4 mm, which corresponds to a decrease between 8% and 7%, it results in a maximal decrease of approximately 52% in k_m at rest. Regarding a decrease in α between 38% and 33%, which likely occurs with knee extension, it results in a maximal decrease of approximately 5% in k_m considering torques between 0 and 20 Nm.

Parameter change	Δk_f (%)				
	T=0 Nm	T=5 Nm	T=10 Nm	T=15 Nm	T=20 Nm
$\alpha - \Delta\alpha$	-4.96	-4.87	-4.82	-4.81	-4.84
$k_t - \Delta k_t$	-71.6	-58.6	-51.1	-46.2	-42.7
$r - \Delta r$	-34.0	-23.4	-19.3	-17.1	-15.7

Table 3.2: Variation in muscle stiffness (Δk_f) with changes in muscle pennation angle (α), which occur with knee extension, and with possible variations in tendon stiffness (k_t) and muscle moment arm length (r) between subjects.

Chapter 4

Discussion

In this section, the results of the SRS model simulations are discussed, as well as the results of the MTC model sensitivity analysis. Possible methodological and equipment limitations will be addressed and several recommendations and ideas for the future will be given.

4.1 Goodness of the SRS model fit

Regarding the measurements done without a subject attached to the manipulator, it is possible to observe in figure 3.1.B a high fluctuation on the measured torque. Due to this fluctuation, the model could not simulate with great accuracy the measured torque, as we can see in figure 3.1.D and by the relatively low VAF values presented in table 3.1, which don't reach 99%. For this reason, despite the low SEM values, the Achilles parameters were not accurately estimated and I_l and b_l had to be adjusted to increase the goodness of the SRS model fits regarding subjects' simulations. The poor estimation of the Achilles parameters could be explained by the somewhat compliance of the footplate, which could be responsible for the torque fluctuation, and by the fact that the manipulator was working near its power limits.

After the adjustment of the Achilles parameters, the subjects' measured displacement and torque were more accurately simulated, as shown in figure 3.2.C and 3.2.D and by the high VAF values in table C.1, in appendix D. Despite the high mean VAF values, the high SEM of some estimated parameters raised doubts about the goodness of the model fits, as it will be described below.

4.2 Reliability of the estimated SRS model parameters

Observing the low SEM values of the Achilles parameters (I_l,b_l and k_l) in table 3.1, we would assume that these were accurately estimated. However, as previously mentioned, they had to be adjusted to improve the SRS model simulations of the subjects' data. In table C.1, in appendix D, it is possible to observe that the mean SEM of the other estimated parameters is relatively low, except for x_s and k_{dec}. This means that the parameters were accurately estimated, excluding x_s and k_{dec}.

Table 4.1 shows the range of the parameters estimated in this study, for both knee angles, and the results obtained by Eesbeek et. al [29] for the wrist, over all torque levels used. The joint inertia (I_j) is approximately 10 times higher for the ankle than for the wrist. Although I_j presented a low SEM, there is also a 10-fold difference from the values reported in literature, which range from 0.00473-0.00543 kg m^2 [52].

The interface damping (b_f) and stiffness (k_f) are considerably higher in this experiment comparing to the wrist results, which might be due to the relatively low stiffness of the footplate and/or a poor attachment between the footplate and the foot. Moreover, the compression applied on the foot skin by the velcro straps was arbitrary and could have also contributed to a higher k_f, since skin stiffness is thought to increase with compression [29].

The estimated muscle SRS (k_{SRS}) is approximately 10 times higher for the leg muscles than for the wrist muscles. This is well correlated with the fact that in this experiment the torque levels used were approximately 10 times higher than those used in the wrist experiment. The same applies to k_{dec}. These parameters, as well as x_e, will be discussed further below.

4.2.1 Variation of the estimated parameters

Considering the parameters ITSTD, illustrated in figure 3.4, they are relatively high except for I_j and k_{SRS}, which are approximately below 0.2. This means that there is a high variation in the estimated parameters with respect to a certain torque level. During the experiment, the velcro straps became slightly loose, which resulted in a poorer attachment between the foot and the footplate across the trials. This may explain the high ITSTD observed. In addiction, when changing the knee angle, sometimes the velcro straps had to be reattached. Relative to k_{dec} and x_e, the high ITSTD values for all torque levels are in accordance with the respective high SEM values. An insufficient rest time between repetitions could have also contributed to higher ITSTD, since muscles might be still recovering from the stretch imposed [29]. Comparing to the results

Parameter range or mean value	KA = 90°	KA = 180°	Eesbeek et. al [29]
I_j (kg m^2)	0.0346-0.0350	0.0348-0.0363	0.0024
b_f (Nm/rad/s)	6-21	8-16	0.62-0.73
k_f (Nm/rad)	1885-3735	1614-3851	77-127
k_{SRS} (Nm/rad)	69-244	72-215	8-22
k_{dec} (Nm/rad)	84-265	97-228	3-12
x_e (rad)	0.022-0.042	0.022-0.031	0.022-0.063

Table 4.1: Comparison between the SRS model estimated parameters range obtained in this study for the ankle, at two different knee angles (KA), and previously obtained by the wrist by Eesbeek et. al [29].

obtained by Eesbeek et. al [29], the ITSTD and SEM values were also higher in this study for most of the estimated parameters.

Regarding the repeated measurements (see figure 3.7), the most consistent parameter was I_j, which is in accordance with the low ITSTD values found. The other parameters were more unstable, as we can conclude by the discrepancy observed between the estimated parameters on different days for the same subjects. It is important to denote that one of the subjects used an extra foot support under the velcro straps on the second day, which was not used in the first measurements. This could explain the lower mean values and SD of b_f, k_f, k_{dec} and x_e and the lower SEM values of these parameters, in general (see figure C.1, in appendix C). Although the SEM values of x_e and k_{dec} are still very high, the SRS model parameters of these two subjects were more accurately estimated on the second day. Therefore, the coupling between the foot and the footplate seems to be determinant in estimating the SRS model parameters. Small differences in the foot and leg positions and the arbitrary tension applied by the velcro straps on the foot may also contribute to this variability.

4.2.2 SRS estimation

As we can observe in figure 3.3.A and 3.3.B, it is possible to observe a transition point in the elastic part of the joint torque ($T_{j,elas}$) against time and as a function of joint displacement (θ_j), respectively, for some torque levels. This is similar to the results obtained previously for the wrist joint (see figure 1.4(a)) [29]. However, in other repetitions this transition point was not so clear, which was related to a poor estimation of the joint parameters (k_{SRS}, x_e and k_{dec}). This could be due to a bad coupling between the foot and the footplate, which results in the estimation of the manipulator's mechanical properties instead of the joint properties. Some subjects

actually reported some difficulty in maintaining the heel in contact with the footplate at higher torques.

The characteristics of the ramp perturbation may also compromise SRS estimation. If the velocity is not high enough, there is a higher probability that some cross-bridges have already de-attached, which would result in an underestimation of k_{SRS} for all torque levels [18]. The peak velocity of ramp perturbation used in this study was limited to 2 rad/s, lower than the 3 rad/s of the ramp used by Eeesbeek et. al [29]. With increasing torque level, the maximum velocity attainable was even lower, reaching approximately only 1.5 rad/s at the 20 Nm torque level (see figure B.2, in appendix B). Hence, the stretch induced on the TS muscles during the time interval used for analysis (55 ms) may have been not large and/or fast enough to accurately estimate SRS. As we can observe in figure 3.2.A, the data used for the model parametrization concerned only the initial part of the ramp perturbation applied.

Kirsch and Kearney [51] estimated ankle stiffness while applying ramp stretches with a superimposed stochastic perturbation. They believed that the ankle stiffness frequency response magnitude at low frequencies (k_{low}) mainly reflects muscle SRS. In this study, subjects generated pre-stretch torques between 13 and 20 Nm and the corresponding k_{low} ranged 203-333 Nm/rad. These values are somewhat higher than the estimated k_{SRS} in this study, which varies from 168 to 244 Nm/rad, considering torque levels between 10 and 20 Nm. This could be due to the characteristics of the ramp used by Kirsch and Kearney [51], which had a duration of only 25 ms and a peak velocity of 6 rad/s. SRS is believed to be independent on the stretch velocity [53], but the velocity has to be high enough, as previously mentioned.

Regarding other equipment limitations, the footplate oscillation could also contribute to mask the transition associated with k_{SRS}. Nevertheless, this effect should not be very significant, considering a good coupling between the foot and the footplate.

4.3 SRS dependence on torque and knee angle

As expected, k_{SRS} increased with torque level for both knee angles, as illustrated in figure 3.5. Assuming that muscle stiffness dominates joint stiffness and that the force generated per cross-bridges is constant, this increase in k_{SRS} with torque level mainly reflects the higher number of cross-bridges attached. The stiffness of passive structures within the muscles or connected in parallel with the muscles, such as the Achilles tendon, may have also contributed to this increase, and thus muscle k_{SRS} might have been overestimated [29]. Notwithstanding, this effect is unlikely to be very significant, considering that the torque levels used in this experiment were relatively low.

Co-contraction, i.e. the simultaneous contraction of agonist and antagonist muscles around a joint to hold a position, also affects the estimated k_{SRS} [54]. By the EMG results (see figure 3.6), it seems that the activity of the TS muscles, the main agonists of plantarflexion, increases with torque level, even though this increase is not very pronounced. On the other hand, TA muscle activity, the main antagonist of plantarflexion, seems to remain at a certain level despite increasing torque. Therefore, although co-contraction might have contributed to an overestimation of k_{SRS}, it does not seem to have a significant influence on the SRS-torque relationship.

Regarding measurements done with the knee extended and flexed at 90°, no significant differences were found in the estimated k_{SRS}. However, k_{SRS} measured with the knee flexed seems to have a tendency to be higher than k_{SRS} measured with the knee extended, which is in accordance with our hypothesis. It was expected that a higher contribution of GM and GL type II fibres, with the knee extended, would result in a lower k_{SRS} since type II fibres seem to be less stiff than type I fibres [21, 22, 23]. From the EMG analysis results, it is not clear though if GM and GL EMG activity is higher with the knee extended, as expected. On the contrary, GM and GL EMG activity seems to be higher regarding measurements performed with the knee flexed than with the knee extended, as we can observe in figure 3.6.

In the same figure, it is possible to observe that the mean normalized EMG values don't reach values higher than 0.5, which suggests that the subjects generated torques relatively below their MVC torques. It was not possible to measure the MVC torques of subjects due to limitations in the equipment, but as reported in literature, the MVC torques of young male subjects reach values over 100 Nm [36, 55, 56] and the maximum torque the subjects were asked to generate was only 20 Nm. Therefore, the torque levels used in this experiment might have been not sufficiently high to elicit a significant recruitment of type II fibres, which could explain that no differences were found in the estimated SRS at different knee angles. This could also explain why the increase in the EMG activity of TS muscles with torque level is not very pronounced. In addiction, the pennation angle of these muscles increases with torque level and knee flexion, which may result in a configurational change of muscle fibres within the recording volume of the EMG electrodes [57] and, consequently, a reduction in the recorded EMG activity. However, this effect should not be very significant, since the torque levels used were considerably low. Moreover, no significant differences were found in the EMG activity measured at different knee angles, which could be explained by an increase in muscles' pennation angle.

The large SD of the mean normalized EMG can be explained by the existence of outliers, which may arise from different MVC torques between subjects or from a dif-

ferent alignment between the electrodes and the muscles' fibres. Although only one subject reported difficulty in completing the task at higher torques, it would be necessary to record the muscles EMG at rest and during MVC to calculate more accurately the normalized EMG and compare the subjects at the same working point level.

In general, the EMG signals contained a lot of noise, observable in the recordings by the continuous presence of a wave with a frequency of 50 Hz, approximately. To reduce the noise, the experiment was performed with the lights turned off but there were still other sources of noise, such as the equipment itself, and artefacts that could not be avoided, derived from the subject movement during the experiment [47]. Despite most of the noise was successfully filtered during the analysis, the artefacts are difficult to remove.

To obtain better EMG recordings, the leg used during the experiment could be shaved, in order to improve the contact between the electrodes and the skin and thus obtain signals with better quality. Furthermore, ultrasound measurements could be used to ensure that the electrodes are aligned with the muscles' fibres orientation at rest and to quantify the changes in pennation angle with torque level and knee flexion. Another method to quantify muscle activity that could be used is intramuscular EMG. Although this technique provides more reliable EMG recordings, it is uncomfortable to the subjects and thus its usage should be carefully discussed.

The hypothesis that muscle fibre type recruitment influences SRS needs to be further investigated. Different protocols could be used to increase the activity of a certain type of fibres, exploring the different properties that fibres exhibit, such as their fatigue response and their different optimal velocity. For example, Stijntjes developed a method to estimate muscles' maximal RP and maximal velocity of the wrist muscles [30]. The protocol to estimate these parameters is similar to the SRS protocol but, instead of applying a ramp rotation, the manipulator is suddenly released and the hand/foot freely rotates in the direction that the subject was generating a determined torque level. After overcoming the velocity limitations of the Achilles manipulator, it would be possible to apply this method to the ankle.

4.4 Elastic limit of cross-bridges

It is possible to relate the elastic limit (x_e), obtained at the joint level, to the sarcomere level, by expressing it in nanometres per half sarcomere (nm p.h.s.) as follows:

$$x_s = \frac{x_e r \cos\alpha}{L_{MTU}} \frac{L_s}{2} \tag{4.1}$$

where x_s is the elastic limit in nm p.h.s., x_e the elastic limit in radians, r the muscle

moment arm length, L_{MTU} the muscle-tendon unit length, α the muscle pennation angle and L_s the sarcomere length.

Considering the values of r, L_{MTU}, α and L_s presented in table 4.2, a mean elastic limit (x_e) of 0.0245 rad and 0.0277 rad relative to a knee angle of 90° and 180° respectively, the mean x_s is approximately 7 nm p.h.s., for both knee angles. This value is slightly lower than the values found in literature regarding experiments done in animals, which range from 8 to 20 [29].

Table 4.2: Moment arm length (r), muscle-tendon unit length (L_{MTU}) and pennation angle, with the knee flexed ($\alpha_{90°}$) and with the knee extended ($\alpha_{180°}$), of gastrocnemius medialis (GM), gastrocnemius lateralis (GL) and soleus (SOL) muscles, the main plantar flexors. This data was used to estimate the elastic limit in nm p.h.s., considering the x_e estimated with the knee flexed ($x_{s,90°}$) and extended ($x_{s,180°}$).

Muscle	r [mm]	L_{MTU} [mm]	$\alpha_{90°}$ [e] [°]	$\alpha_{180°}$ [f] [°]	L_s [g] [μm]	$x_{s,90°}$ [nm p.h.s.]	$x_{s,180°}$ [nm p.h.s.]
GM	63[a]		23	19	2.71	7.30	7.66
GL	64[b]	302[d]	15	13	2.71	7.77	8.01
SOL	66[c]		27	27	2.31	6.29	6.43

[a] [48] [b] [36] [c] [35] [d] [58] [e] [50] [f] [50, 33] [g] [59]

Comparing to the mean value obtained for the wrist muscles (0.066 rad), the x_e obtained in this study for the leg muscles is more than two times lower. The mean x_s is also approximately two times lower than the estimated value for the wrist (16 nm p.h.s.) [29]. This might be due to the velocity of the ramp perturbation applied, since x_e was found to be dependent on joint velocity [53]. It is also important to remind that the SEM values of this parameter were very high, which means that x_e was not accurately estimated. At zero torque level, x_e is slightly higher than for the other torque levels, as we can observe in table C.1, in appendix C. This is likely because the ramp velocity could not achieve its maximum velocity (2 rad/s) at higher torque levels, as previously mentioned.

4.5 Contribution of tendon stiffness and pennation angle to SRS

In relation to the results of the MTC model (see table 3.2), the parameter that has the greatest variation, between subjects, is tendon stiffness (k_t) and thus, it has the biggest influence on muscle stiffness (k_m). Therefore, it might be important to include the contribution of the tendon in the SRS model, by adding another component. It could also be included, during the experiment, a method to estimate tendon stiffness,

such as the tendon travel method, which involves the estimation of tendon elongation [60, 48].

According to our hypothesis, an increase in knee flexion, and thus in muscles' pennation angle (α), would contribute to a lower estimated muscle SRS. However, according to the MTC model, a decrease in α results in a lower k_m. Nevertheless, the highest contribution in k_m expected from a considerable change in α is 5% and, the differences found between the estimated k_{SRS} at different knee angles ranged 1-12%.

Regarding muscle moment arm length (r), a reduction in its value also contributes to a reduction in k_m, being this reduction more significant at lower torques. Therefore, anatomical differences between subjects might contribute to differences in k_{SRS}, as previously mentioned. The influence of r on k_m also emphasizes the importance of a good alignment between the ankle centre of rotation and the motor axis.

Chapter 5

Conclusion

Muscle mechanical properties are one of the main determinants of joint performance *in vivo*. Several conditions, such as prolonged immobilization, ageing, type 2 diabetes and neuromuscular diseases may result in changes in muscle mechanics, influencing patients mobility and consequently, their quality of life. These changes might be seen at the molecular level, such as a reduction in the number of cross-bridges, believed to happen with ageing, or at the muscle level, such as changes in muscle fibre type composition. Moreover, specific exercise training is believed to contribute to overcome this changes. Therefore, there is a need to develop non-invasive methods to estimate muscle mechanics *in vivo*, in order to evaluate patients quantitatively and provide them a more accurate diagnostic and follow up. These techniques could also be applied to evaluate the consequences of different specific exercise training in patients or high level performance sports.

In this study, an haptic manipulator was used to impose fast ramp perturbations to the ankle joint in the dorsiflexion direction, while subjects were generating a determined torque level in the opposite direction. From the measured torque and displacement, and using a mechanical model previously developed by Eesbeek et. al [29], leg muscles SRS was estimated. This parameter is believed to reflect mainly the stiffness of attached cross-bridges and thus it might be important to evaluate the muscle properties of patients with the conditions previously mentioned. Furthermore, SRS is believed to differ between fibre types. Differences in the estimated SRS at different knee angles could reflect the different composition of the leg muscles in terms of fibre types.

Despite other parameters of the model were not accurately estimated, the model seems adequate to estimate leg muscles SRS. Regarding measurements done with the knee flexed and extended, no statistically significant differences were found in the estimated SRS. This could be explained by the low torque levels applied or the characteristics of the ramp perturbation used. In order to confirm these results, several equipment

and methodological changes should be made, such as: increase the motor's power, increase the stiffness of the footplate and improve the attachment between the footplate and the foot. In general, these changes would likely provide a better estimation of the SRS model parameters.

By overcoming the power limitation of Achilles, it would be possible to apply faster ramps at higher torque levels, measure MVC torque and estimate SRS at different % of MVC, which would allow the comparison of subjects at the same working point level. Moreover, other relevant mechanical parameters could be estimated, such as maximal RP and the velocity at maximal RP, as previously done for the wrist muscles [30]. The RP protocol was not included in this study because Achilles' velocity was limited to 2 rad/s and we would expect velocities at least ten times higher.

From the sensitivity analysis of the MTC model, Achilles tendon stiffness has an appreciable variability between subjects, which might contribute to the variance of the estimated muscle stiffness. Therefore, it may be relevant to include another component on the SRS model to discriminate between muscle and tendon stiffness. This would likely provide a better estimation of SRS. Ultrasonography could be used to measure tendon elongation and estimate Achilles tendon stiffness [48, 60, 61]. Furthermore, additional components could be included in the model to discriminate the contribution of the different muscles to SRS, as previously suggested by Eesbeek et. al [29]. To measure muscle activity more precisely, surface EMG could be used together with ultrasound measurements, which would enable a better alignment between the electrodes and muscles' fibres and to measure the changes in muscles' pennation angle with increasing torque or knee flexion. Although it is more uncomfortable to the subjects, intramuscular EMG could also be used for this purpose.

In conclusion, SRS is an important parameter to characterize muscle mechanics. More research is needed to improve the method to estimate it *in vivo*, which includes equipment improvements, and to investigate whether SRS can provide information about muscle fibre type composition. SRS might be important not only to evaluate changes at muscle level, due to several conditions and diseases, but also changes in Achilles stiffness, which occur with ageing [62] or as a result of certain diseases or injuries. In the future, different protocols may be developed to explore other properties that distinguish muscle fibre types, such as their resistance to fatigue and their power-velocity relationships. In addiction, other populations could be measured, including female, elderly and patients with altered muscle fibre composition or altered tendon stiffness. It would also be interesting to investigate a population with a clinical history of falling, since SRS is thought to be important in balance maintenance after rapid perturbations [18].

Appendices

Appendix A

SRS model

The SRS model developped by Eesbeek et. al [29], represented in figure 1.5, is fully described by the next set of differential equations:

$$I_l\ddot{\theta}_l = (\dot{\theta}_m - \dot{\theta}_l)b_l + (\theta_m - \theta_l)k_l - (\dot{\theta}_l - \dot{\theta}_j)b_f + (\theta_l - \theta_j)k_f \tag{A.1}$$

$$I_j\ddot{\theta}_j = (\dot{\theta}_l - \dot{\theta}_j)b_j + (\theta_l - \theta_j)k_j - \dot{\theta}_j b_j - \theta_j k_j \tag{A.2}$$

Joint stiffness (k_j) was modelled has having a bi-phasic non-linear behaviour, as represented in figure A.1, and it was implemented by a logarithmic function:

$$k_j = k_{SRS} - \log[1 + \exp(a_s k_{dec}(\theta_j - x_e))]/a_s \tag{A.3}$$

where a_s is a fixed smoothness parameter for the stiffness transition at x_e, which was assumed to be 100. In table A.1 all the model parameters are described along with their units.

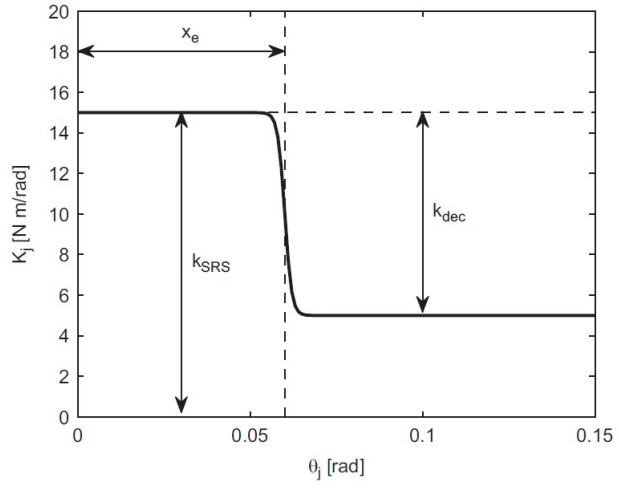

Figure A.1: Bi-phasic modelled behaviour of joint stiffness (k_j). Figure taken from [29].

Parameter	Description	Units
	Subsystem I	
I_l	manipulators' inertia	kg m^2
b_l	manipulators' damping	N m s/rad
k_l	manipulators' stiffness	N m/rad
	Subsystem II	
b_f	foot-manipulator interface damping	N m s/rad
k_f	foot-manipulator interface stiffness	N m/rad
	Subsystem III	
I_j	joint inertia	kg m^2
k_{SRS}	short-range stiffness (SRS)	N m/rad
k_{dec}	stiffness beyond elastic limit (decrement to k_{SRS})	N m/rad
x_e	elastic limit	rad

Table A.1: Description of the parameters that characterize the different subsystems of the SRS model. Table adapted from [29].

Appendix B

Achilles raw data

In this appendix, it is possible to observe the raw data collected with the Achilles manipulator relative to subjects. In table B.1, we can see the raw torques of all subjects, measured at different initial torque levels, with the flexed at 90°, that were used for parametrization. The time window analysis width was 55 ms and the initial torques were subtracted from the traces. In figure B.1, we can see the mean measured torques, for the different torque levels, at both knee angles. In table B.2, it is possible to observe an example of the commanded, measured and filtered displacement, velocity and acceleration of one subject at two different torque levels, with the knee flexed at 90°. Similar results were obtained with the knee extended (180°).

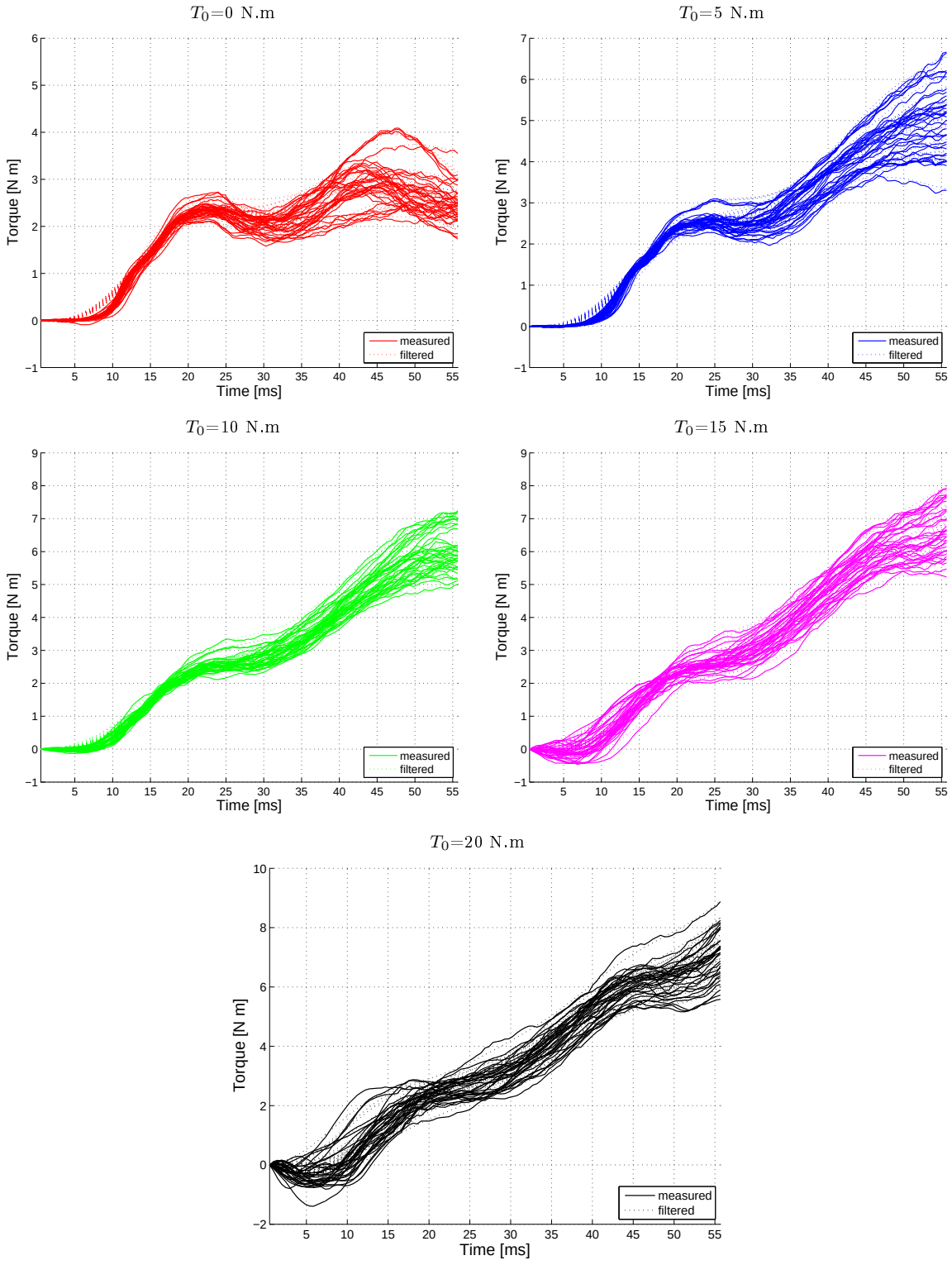

Table B.1: Raw measured torques of all subjects, used for the SRS model optimization, for the different torque levels. The initial torque was subtracted from the traces.

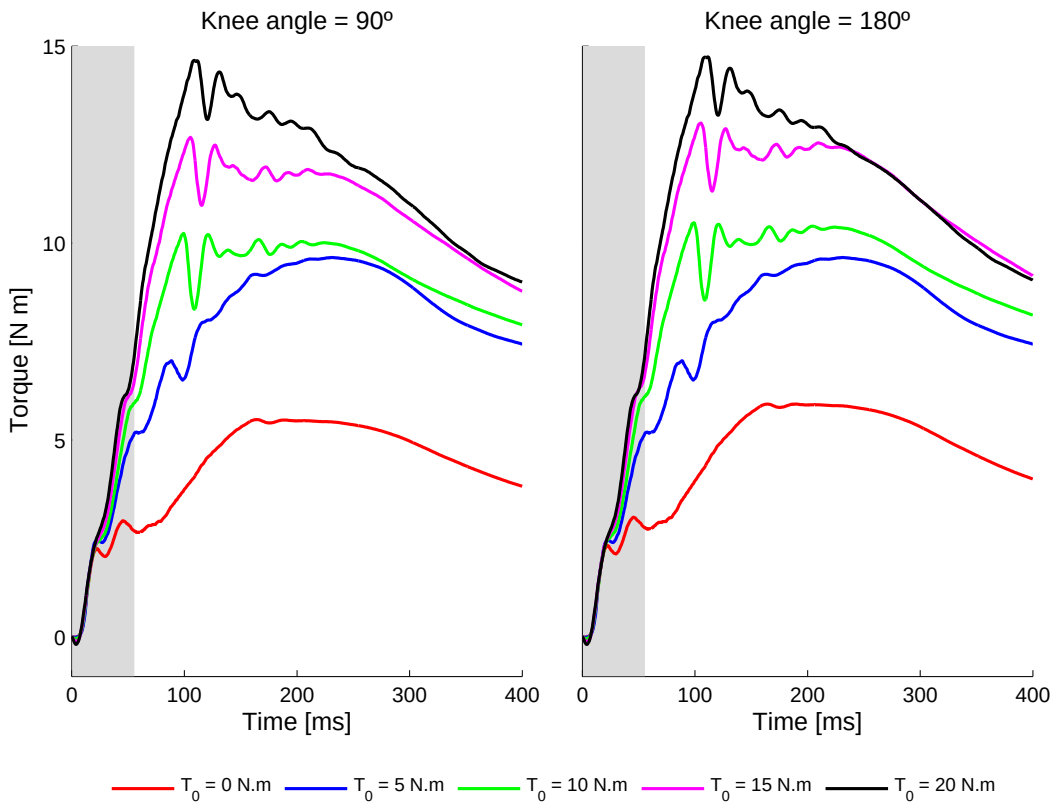

Figure B.1: Measured torque, averaged over subjects, for the different torque levels and for both knee angles. The grey area denotes the time window used for the SRS model parameters estimation. The mean initial torque was subtracted from the traces.

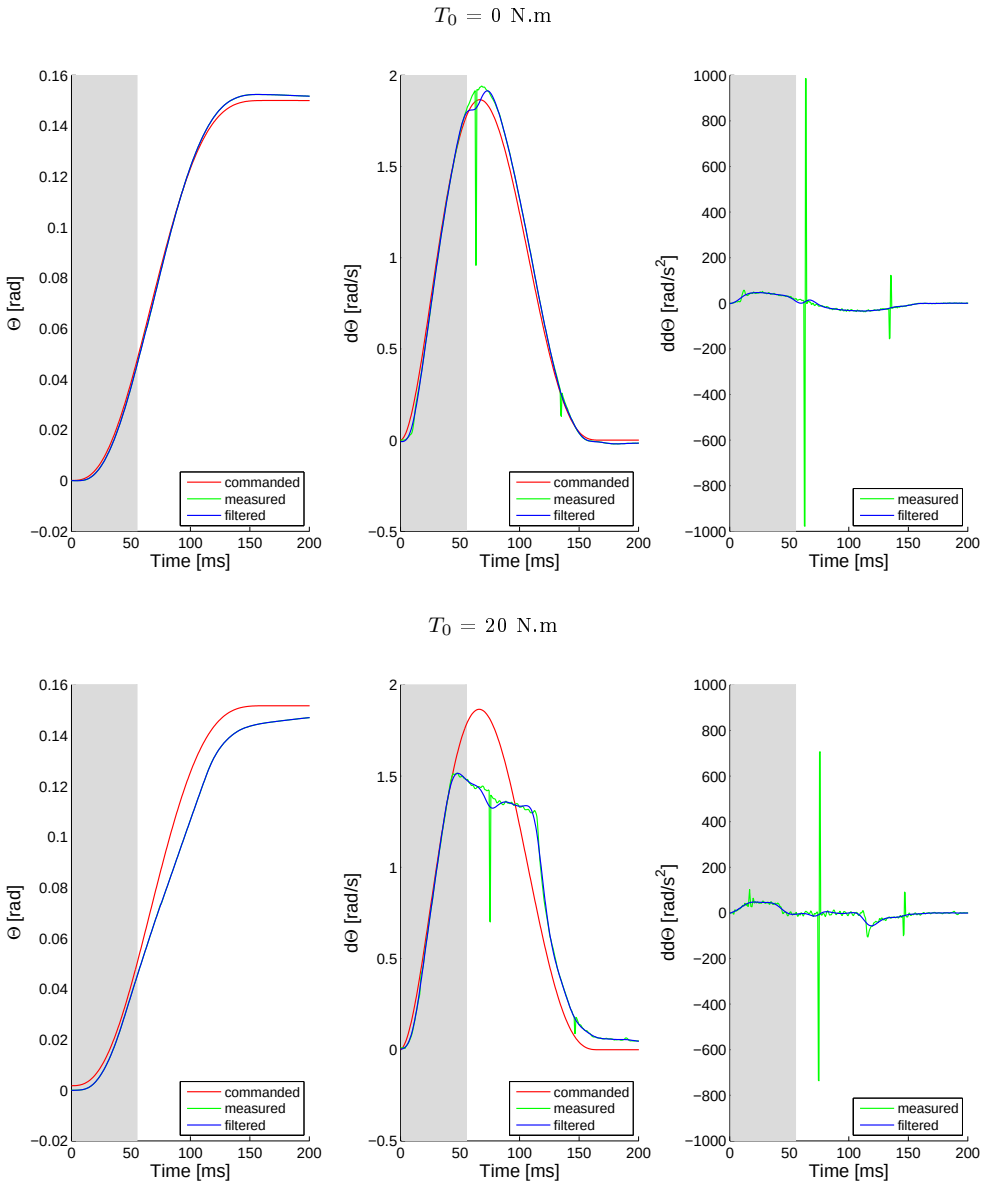

Table B.2: Example of the commanded, measured and filtered displacement, velocity and acceleration of one subject repetition for all torque levels, at a knee angle of 90°. The grey area denotes the time window used for the SRS model parameters estimation. The initial position was subtracted from the displacement traces.

Appendix C

Estimated parameters of the SRS model

In table C.1, it is possible to observe the mean values ± SEM of the estimated SRS model parameters at all torques levels and both knee angles. Regarding repeatability analysis, we can see in figure C.1 the mean SEM values of the estimated parameters of the two subjects, measured on different days.

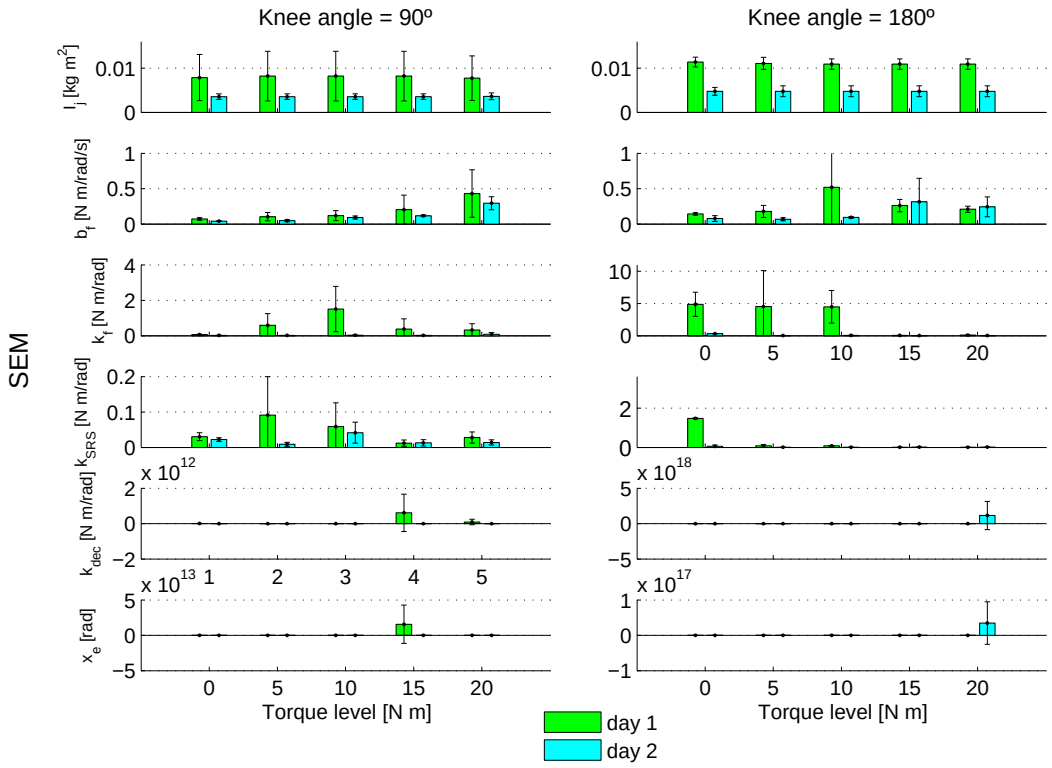

Figure C.1: Mean SEM values of the estimated SRS model parameters of two subjects, measured on two different days with the knee flexed at 90° and extended (180°).

Knee angle = 90°					
Parameter value ± SEM	$T_0 = 0$ Nm	$T_0 = 5$ Nm	$T_0 = 10$ Nm	$T_0 = 15$ Nm	$T_0 = 20$ Nm
I_j (kg m^2)	0.0350 ± 0.0082	0.0346 ± 0.0080	0.0346 ± 0.0080	0.0348 ± 0.0082	0.0348 ± 0.0082
b_f (N m s/rad)	5.5787 ± 0.1119	6.2967 ± 0.1699	5.4146 ± 0.1947	9.4289 ± 0.2025	21.0648 ± 0.4391
k_f (N m/rad)	1.8854×10^3 ± 0.3865	1.9097×10^3 ± 0.6151	1.8513×10^3 ± 0.9130	2.5117×10^3 ± 1.4318	3.7346×10^3 ± 0.1597
k_{SRS} (N m/rad)	68.5002 ± 0.0385	149.3359 ± 0.0792	181.7193 ± 0.0541	209.7807 ± 0.0242	244.0790 ± 0.0171
k_{dec} (N m/rad)	84.2213 ± 4.0576×10^9	180.2452 ± 1.2027×10^9	272.4758 ± 1.5451×10^{11}	176.7356 ± 1.2313×10^{11}	264.5676 ± 1.8099×10^{10}
x_e (rad)	0.0421 ± 1.4120×10^8	0.0259 ± 1.1549×10^8	0.0255 ± 1.7137×10^{10}	0.0222 ± 3.1288×10^{12}	0.0242 ± 7.3666×10^9
VAF (%)	99.7978	99.9304	99.9492	99.8828	99.6029
T_0 (N m)	1.7231	4.9972	9.9491	14.7802	19.6946
Knee angle = 180°					
Parameter value ± SEM	$T_0 = 0$ Nm	$T_0 = 5$ Nm	$T_0 = 10$ Nm	$T_0 = 15$ Nm	$T_0 = 20$ Nm
I_j (kg m^2)	0.0363 ± 0.0056	0.0358 ± 0.0055	0.0357 ± 0.0054	0.0358 ± 0.0055	0.0348 ± 0.0069
b_f (N m s/rad)	7.9147 ± 0.0692	7.1175 ± 0.0658	7.1263 ± 0.0991	9.0431 ± 0.1703	16.1058 ± 0.3248
k_f (N m/rad)	1.6144×10^3 ± 0.7251	1.8716×10^3 ± 0.4603	1.8783×10^3 ± 0.5781	2.8723×10^3 ± 0.4668	3.8512×10^3 ± 0.1104
k_{SRS} (N m/rad)	72.3693 ± 0.0494	131.0900 ± 0.0194	168.6682 ± 0.0354	212.5100 ± 0.0296	215.7540 ± 0.0134
k_{dec} (N m/rad)	97.1537 ± 2.0275×10^6	212.5415 ± 3.2677×10^{18}	235.4563 ± 6.1530×10^{15}	98.7481 ± 1.5388×10^9	228.1109 ± 1.0873×10^{11}
x_e (rad)	0.0312 ± 1.5355×10^8	0.0306 ± 2.8675×10^{17}	0.0300 ± 5.7755×10^{14}	0.0217 ± 1.6822×10^8	0.0286 ± 3.7071×10^{10}
VAF (%)	99.8051	99.8817	99.9049	99.9528	99.7875
T_0 (N m)	2.1185	5.0211	9.8700	14.7832	19.5404

Table C.1: Mean estimated parameters and corresponding SEM values, averaged over subjects, for each torque level and regarding both knee angles used in the experiment. It is also possible to observe the mean VAF of the model fits and the mean initial measured torque (T_0).

Appendix D

EMG raw data and analysis

In this appendix, it is possible to observe an example of the EMG recordings of the SOL, GM, GL and TA muscles during the SRS experiment in figure D.1. The EMG system and the Achilles were connected and the square wave signal, observed in the first plot, indicates the time interval during which the ramp stretch was applied. A time window of 500 ms was used to calculate the mean EMG activity of the subjects prior to the ramp perturbation, which starts at $t = 0$. For the 0 N.m torque level, a time window of 200 ms was used since the ramp perturbation was automatically applied 0.5 s after the beginning of the trial.

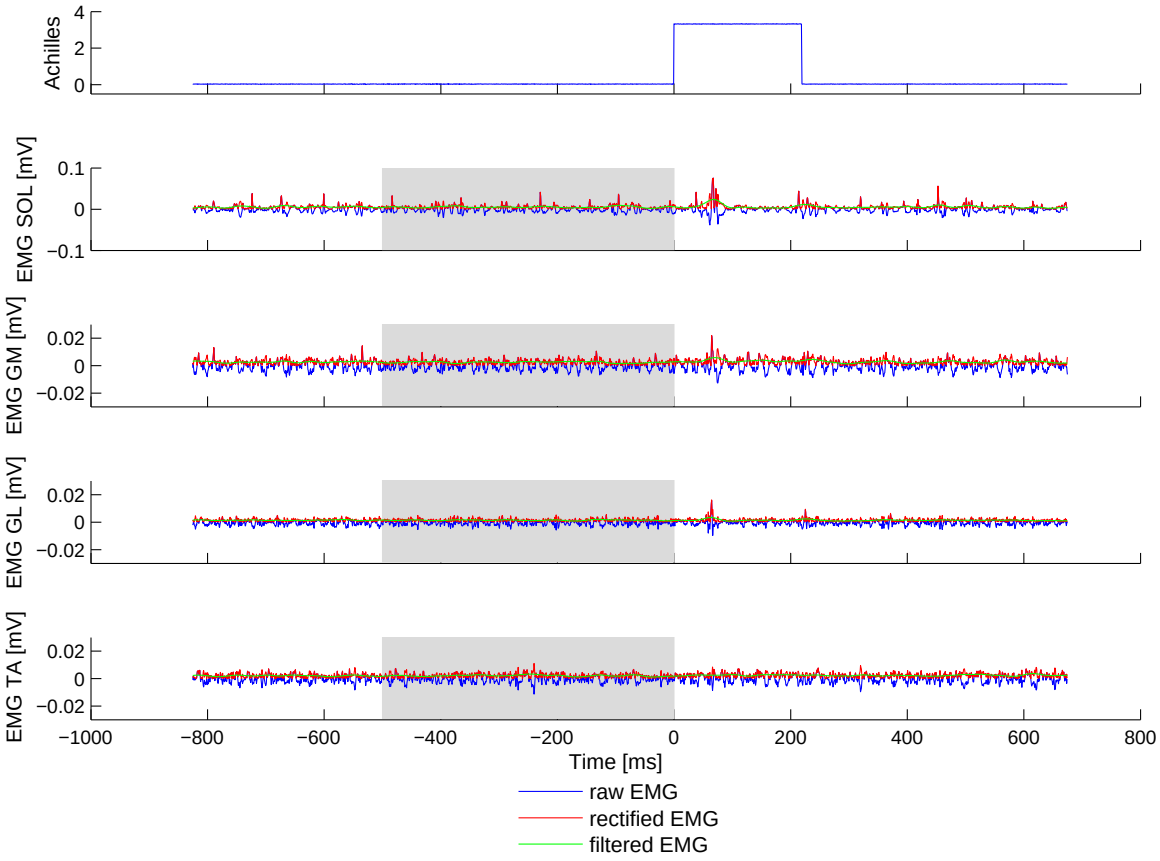

Figure D.1: Example of the raw (in blue), rectified (in green) and filtered (in red) EMG data of the SOL, GM, GL and TA muscles during the SRS experiment, at a torque level of 5 N m. In the first plot, the square wave indicates when the ramp perturbation occurred. It is possible to observe that the TS muscles reflexes appeared later than 50 ms after the ramp stretch had started. The grey area denotes the time window used to calculate the mean normalized EMG ($\overline{EMG}_n$).

Bibliography

[1] S. Schiaffino and C. Reggiani, "Fiber types in mammalian skeletal muscles," *Physiological Reviews*, vol. 91, no. 4, pp. 1447–1531, 2011.

[2] B. Lowell and G. Shulman, "Mitochondrial dysfunction and type 2 diabetes," *Science*, vol. 307, no. 5708, p. 384, 2005.

[3] K. Petersen, S. Dufour, D. Befroy, R. Garcia, and G. Shulman, "Impaired mitochondrial activity in the insulin-resistant offspring of patients with type 2 diabetes," *New England Journal of Medicine*, vol. 350, no. 7, pp. 664–671, 2004.

[4] J. Andersen, T. Gruschy-Knudsen, C. Sandri, L. Larsson, and S. Schiaffino, "Bed rest increases the amount of mismatched fibers in human skeletal muscle," *Journal of Applied Physiology*, vol. 86, no. 2, p. 455, 1999.

[5] E. Borina, M. Pellegrino, G. D'Antona, and R. Bottinelli, "Myosin and actin content of human skeletal muscle fibers following 35 days bed rest," *Scandinavian journal of medicine & science in sports*, vol. 20, no. 1, pp. 65–73, 2010.

[6] P. Aagaard, J. Andersen, M. Bennekou, B. Larsson, J. Olesen, R. Crameri, S. Magnusson, and M. Kjær, "Effects of resistance training on endurance capacity and muscle fiber composition in young top level cyclists," *Scandinavian journal of medicine & science in sports*, 2011.

[7] A. Kryger and J. Andersen, "Resistance training in the oldest old: consequences for muscle strength, fiber types, fiber size, and mhc isoforms," *Scandinavian journal of medicine & science in sports*, vol. 17, no. 4, pp. 422–430, 2007.

[8] L. Verdijk, B. Gleeson, R. Jonkers, K. Meijer, H. Savelberg, P. Dendale, and L. van Loon, "Skeletal muscle hypertrophy following resistance training is accompanied by a fiber type–specific increase in satellite cell content in elderly men," *The Journals of Gerontology Series A: Biological Sciences and Medical Sciences*, vol. 64, no. 3, p. 332, 2009.

[9] D. Williamson, M. Godard, D. Porter, D. Costill, and S. Trappe, "Progressive resistance training reduces myosin heavy chain coexpression in single muscle fibers from older men," *Journal of Applied Physiology*, vol. 88, no. 2, pp. 627–633, 2000.

[10] A. Baguet, I. Everaert, P. Hespel, M. Petrovic, E. Achten, and W. Derave, "A new method for non-invasive estimation of human muscle fiber type composition," *PLoS ONE*, vol. 6, no. 7, p. e21956, 2011.

[11] W. Scott, J. Stevens, and S. Binder–Macleod, "Human skeletal muscle fiber type classifications," *Physical therapy*, vol. 81, no. 11, p. 1810, 2001.

[12] J. Andersen, "Muscle fibre type adaptation in the elderly human muscle," *Scandinavian journal of medicine & science in sports*, vol. 13, no. 1, pp. 40–47, 2003.

[13] H. Klitgaard, M. Zhou, S. Schiaffino, R. Betto, G. Salviati, and B. Saltin, "Ageing alters the myosin heavy chain composition of single fibres from human skeletal muscle," *Acta physiologica scandinavica*, vol. 140, no. 1, pp. 55–62, 1990.

[14] R. Bottinelli and C. Reggiani, "Human skeletal muscle fibres: molecular and functional diversity," *Progress in biophysics and molecular biology*, vol. 73, no. 2-4, pp. 195–262, 2000.

[15] J. Bonny, M. Zanca, O. Boespflug-Tanguy, V. Dedieu, S. Joandel, and J. Renou, "Characterization in vivo of muscle fiber types by magnetic resonance imaging," *Magnetic resonance imaging*, vol. 16, no. 2, pp. 167–173, 1998.

[16] R. Dahmane, S. Djordjevic, B. Simunic, and V. Valencic, "Spatial fiber type distribution in normal human muscle:: Histochemical and tensiomyographical evaluation," *Journal of biomechanics*, vol. 38, no. 12, pp. 2451–2459, 2005.

[17] R. Bottinelli, M. Canepari, M. Pellegrino, and C. Reggiani, "Force-velocity properties of human skeletal muscle fibres: myosin heavy chain isoform and temperature dependence," *The Journal of Physiology*, vol. 495, no. Pt 2, pp. 573–586, 1996.

[18] P. Rack and D. Westbury, "The short range stiffness of active mammalian muscle and its effect on mechanical properties," *The Journal of Physiology*, vol. 240, no. 2, pp. 331–350, 1974.

[19] B. Walmsley and U. Proske, "Comparison of stiffness of soleus and medial gastrocnemius muscles in cats," *Journal of Neurophysiology*, vol. 46, no. 2, p. 250, 1981.

[20] L. Cui, *Quantifying structural and activation-dependent contributions to short-range stiffness of skeletal muscles*. PhD thesis, Northwestern University, 2008.

[21] U. Proske and P. Rack, "Short-range stiffness of slow fibers and twitch fibers in reptilian muscle," *American Journal of Physiology–Legacy Content*, vol. 231, no. 2, pp. 449–453, 1976.

[22] J. Petit, G. Filippi, F. Emonet-Denand, C. Hunt, and Y. Laporte, "Changes in muscle stiffness produced by motor units of different types in peroneus longus muscle of cat," *Journal of Neurophysiology*, vol. 63, no. 1, pp. 190–197, 1990.

[23] J. Malamud, R. Godt, and T. Nichols, "Relationship between short-range stiffness and yielding in type-identified, chemically skinned muscle fibers from the cat triceps surae muscles," *Journal of Neurophysiology*, vol. 76, no. 4, pp. 2280–2289, 1996.

[24] J. Gregory, A. Luff, D. Morgan, and U. Proske, "The stiffness of amphibian slow and twitch muscle during high speed stretches," *Pflügers Archiv European Journal of Physiology*, vol. 375, no. 2, pp. 207–211, 1978.

[25] C. Huyghues-Despointes, T. Cope, and T. Nichols, "Intrinsic properties and reflex compensation in reinnervated triceps surae muscles of the cat: effect of activation level," *Journal of Neurophysiology*, vol. 90, no. 3, pp. 1537–1546, 2003.

[26] L. Cui, E. Perreault, and T. Sandercock, "Motor unit composition has little effect on the short-range stiffness of feline medial gastrocnemius muscle," *Journal of Applied Physiology*, vol. 103, no. 3, p. 796, 2007.

[27] A. Schouten, E. de Vlugt, J. Van Hilten, and F. van der Helm, "Design of a torque-controlled manipulator to analyse the admittance of the wrist joint," *Journal of neuroscience methods*, vol. 154, no. 1-2, pp. 134–141, 2006.

[28] V. Hayward, O. Astley, M. Cruz-Hernandez, D. Grant, and G. Robles-De-La-Torre, "Haptic interfaces and devices," *Sensor Review*, vol. 24, no. 1, pp. 16–29, 2004.

[29] S. van Eesbeek, J. de Groot, F. van der Helm, and E. de Vlugt, "In vivo estimation of the short-range stiffness of cross-bridges from joint rotation," *Journal of biomechanics*, vol. 43, no. 13, pp. 2539–2547, 2010.

[30] M. Stijntjes, "Muscle ageing assessment using wrist neuromechanics," 2011.

[31] L. Systems, "Interactive atlas of human anatomy v.3.0," 2004.

[32] P. Gollnick, B. Sjödin, J. Karlsson, E. Jansson, and B. Saltin, "Human soleus muscle: a comparison of fiber composition and enzyme activities with other leg muscles," *Pflügers Archiv European Journal of Physiology*, vol. 348, no. 3, pp. 247–255, 1974.

[33] Y. Kawakami, Y. Ichinose, and T. Fukunaga, "Architectural and functional features of human triceps surae muscles during contraction," *Journal of Applied Physiology*, vol. 85, no. 2, p. 398, 1998.

[34] M. Narici, T. Binzoni, E. Hiltbrand, J. Fasel, F. Terrier, and P. Cerretelli, "In vivo human gastrocnemius architecture with changing joint angle at rest and during graded isometric contraction," *The Journal of Physiology*, vol. 496, no. Pt 1, p. 287, 1996.

[35] C. Maganaris, "Force–length characteristics of in vivo human skeletal muscle," *Acta physiologica scandinavica*, vol. 172, no. 4, pp. 279–285, 2001.

[36] C. Maganaris, "Force-length characteristics of the in vivo human gastrocnemius muscle," *Clinical anatomy*, vol. 16, no. 3, pp. 215–223, 2003.

[37] D. Rassier, B. MacIntosh, and W. Herzog, "Length dependence of active force production in skeletal muscle," *Journal of Applied Physiology*, vol. 86, no. 5, pp. 1445–1457, 1999.

[38] P. Hodges, L. Pengel, R. Herbert, and S. Gandevia, "Measurement of muscle contraction with ultrasound imaging," *Muscle & nerve*, vol. 27, no. 6, pp. 682–692, 2003.

[39] A. Arampatzis, K. Karamanidis, S. Stafilidis, G. Morey-Klapsing, G. DeMonte, and G. Bruggemann, "Effect of different ankle-and knee-joint positions on gastrocnemius medialis fascicle length and emg activity during isometric plantar flexion," *Journal of biomechanics*, vol. 39, no. 10, pp. 1891–1902, 2006.

[40] K. Hébert-Losier, A. Schneiders, J. García, S. Sullivan, and G. Simoneau, "Peak triceps surae muscle activity is not specific to knee flexion angles during mvic," *Journal of Electromyography and Kinesiology*, 2011.

[41] P. Kennedy and A. Cresswell, "The effect of muscle length on motor-unit recruitment during isometric plantar flexion in humans," *Experimental brain research*, vol. 137, no. 1, pp. 58–64, 2001.

[42] H. Miaki, F. Someya, and K. Tachino, "A comparison of electrical activity in the triceps surae at maximum isometric contraction with the knee and ankle at various angles," *European journal of applied physiology and occupational physiology*, vol. 80, no. 3, pp. 185–191, 1999.

[43] J. Signorile, B. Applegate, M. Duque, N. Cole, and A. Zink, "Selective recruitment of the triceps surae muscles with changes in knee angle," *The Journal of Strength & Conditioning Research*, vol. 16, no. 3, p. 433, 2002.

[44] E. Henneman, G. Somjen, and D. Carpenter, "Functional significance of cell size in spinal motoneurons," *Journal of Neurophysiology*, vol. 28, no. 3, pp. 560–580, 1965.

[45] L. Mendell, "The size principle: a rule describing the recruitment," *J Neurophysiol*, vol. 93, pp. 3024–3026, 2005.

[46] S. E. for the Non-Invasive Assessment of Muscles (SENIAM), "Recommendations for sensor locations in lower leg or foot muscles," Acessed February 10th 2012. `http://www.seniam.org`.

[47] C. De Luca, L. Donald Gilmore, M. Kuznetsov, and S. Roy, "Filtering the surface emg signal: Movement artifact and baseline noise contamination," *Journal of biomechanics*, vol. 43, no. 8, pp. 1573–1579, 2010.

[48] C. Maganaris and J. Paul, "Tensile properties of the in vivo human gastrocnemius tendon," *Journal of biomechanics*, vol. 35, no. 12, pp. 1639–1646, 2002.

[49] C. Maganaris, V. Baltzopoulos, and A. Sargeant, "Changes in achilles tendon moment arm from rest to maximum isometric plantarflexion: in vivo observations in man," *The Journal of Physiology*, vol. 510, no. 3, pp. 977–985, 1998.

[50] C. Maganaris, V. Baltzopoulos, and A. Sargeant, "In vivo measurements of the triceps surae complex architecture in man: implications for muscle function," *The Journal of Physiology*, vol. 512, no. 2, pp. 603–614, 1998.

[51] R. Kirsch and R. Kearney, "Identification of time-varying stiffness dynamics of the human ankle joint during an imposed movement," *Experimental brain research*, vol. 114, no. 1, pp. 71–85, 1997.

[52] A. El Helou, J. Gracies, P. Decq, and W. Skalli, "Estimating foot inertial parameters: A new regression approach," *Clinical biomechanics*, 2011.

[53] E. de Vlugt, S. van Eesbeek, P. Baines, J. Hilte, C. Meskers, and J. de Groot, "Short range stiffness elastic limit depends on joint velocity," *Journal of biomechanics*, 2011.

[54] I. Van der Greft, "Sort range stiffness during voluntary contraction," 2011.

[55] B. Dalton, G. Power, A. Vandervoort, and C. Rice, "Power loss is greater in old men than young men during fast plantar flexion contractions," *Journal of Applied Physiology*, vol. 109, no. 5, p. 1441, 2010.

[56] E. Simoneau, A. Martin, and J. Van Hoecke, "Effects of joint angle and age on ankle dorsi-and plantar-flexor strength," *Journal of Electromyography and Kinesiology*, vol. 17, no. 3, pp. 307–316, 2007.

[57] A. Cresswell, W. Löscher, and A. Thorstensson, "Influence of gastrocnemius muscle length on triceps surae torque development and electromyographic activity in man," *Experimental brain research*, vol. 105, no. 2, pp. 283–290, 1995.

[58] K. Karamanidis and A. Arampatzis, "Mechanical and morphological properties of different muscle–tendon units in the lower extremity and running mechanics: effect of aging and physical activity," *Journal of experimental biology*, vol. 208, no. 20, p. 3907, 2005.

[59] A. Cutts, "The range of sarcomere lengths in the muscles of the human lower limb," *Journal of anatomy*, vol. 160, p. 79, 1988.

[60] C. Maganaris and J. Paul, "Load-elongation characteristics of in vivo human tendon and aponeurosis," *Journal of experimental biology*, vol. 203, no. 4, pp. 751–756, 2000.

[61] T. Muraoka, T. Muramatsu, T. Fukunaga, and H. Kanehisa, "Elastic properties of human achilles tendon are correlated to muscle strength," *Journal of Applied Physiology*, vol. 99, no. 2, p. 665, 2005.

[62] N. Reeves, M. Narici, and C. Maganaris, "Myotendinous plasticity to ageing and resistance exercise in humans," *Experimental physiology*, vol. 91, no. 3, pp. 483–498, 2006.